Nano Research
2023, 16(9): 11783–11800

ISSN 1998-0124 CN 11-5974/O4
https://doi.org/10.1007/s12274-023-5834-4

Review Article

Enhancing the powering ability of triboelectric nanogenerator through output signal's management strategies

Changxin Qi[§], Zhenyue Yang[§], Jinyan Zhi, Ruichao Zhang, Juan Wen (✉), and Yong Qin (✉)

Institute of Nanoscience and Nanotechnology, School of Materials and Energy, Lanzhou University, Lanzhou 730000, China
[§] *Changxin Qi and Zhenyue Yang contributed equally to this work.*

Received: 3 March 2023 / **Revised:** 28 April 2023 / **Accepted:** 15 May 2023

ABSTRACT

As a new branch of efficient and low-cost mechanical energy conversion technology, triboelectric nanogenerator (TENG) is a potential solution to provide a long-term power supply for the Internet of Things (IoT) sensors and portable electronic devices. However, due to inherent working properties of TENG itself such as extremely high internal impedance, pulse, and alternating current (AC) output, TENG can not directly supply power to loads such as batteries efficiently. Based on these, we describe TENG's performance from a new perspective of powering ability. It consists of two aspects: the ability to transport charge effectively and the ability to output high power quality current steadily. In order to push forward the developments and applications of TENG, it is necessary to improve its power supply capacity from different perspectives. Fortunately, in recent years, a variety of output signal's management strategies aiming at effectively managing the generated electricity and significantly improving powering ability of TENG have obtained significantly progress. Herein, this paper discusses the working mechanisms and different load characteristics of TENG at first to clarify the electric performance of TENG. Then, on basis of theoretical analysis, the output signal's management strategies are elaborated from four aspects: improving the cycle output electricity of TENG, increasing the surface charge density of TENG, improving the power quality of TENG-based energy harvesting system, promoting the application of TENG through integrated circuit (IC) technology and TENG network, and the relevant principles and applications are discussed systematically. Finally, the advantages and disadvantages of the above output signal's management strategies are summarized and discussed, and the future development of the output signal's management strategies for TENG is prospected.

KEYWORDS

triboelectric nanogenerator (TENG), inherent working properties, TENG-based energy harvesting system, powering ability, output signal's management strategies.

1 Introduction

In recent years, the emerging technologies such as Internet of Things (IoT) and wearable electronics have developed rapidly and attracted vast attention [1–4]. Widely distributed sensor networks and intelligent wearable electronics with features of flexibility and conformability are believed to completely reshape people's lifestyle. However, for these emerging devices, finding a suitable and sustainable power source is a key challenge. In view of the large amount and wide distribution of the electronic devices in sensor networks, it is no longer feasible to use electricity from the grid. Batteries or capacitors have a limited capacity and need to be recharged and replaced frequently, making maintenance expensive and stressful [5–8]. In addition, the toxic chemicals in the battery would also bring potential environmental risks [6, 9–12]. Therefore, it is urgent to develop sustainable, portable, and environmentally friendly energy solutions for these devices.

Harvesting energy from the surrounding environment and converting it into electricity is a very promising solution. There are many kinds of energy in different environments, such as heat energy [13–16], water energy [17–22], wind energy [23–25], and so on Therefore, in order to make effective use of these widely distributed and diverse environmental energy, energy harvesters have been invented [8]. The energy harvesters can continuously collect environmental energy in a semi-permanent way, and would not pollute the environment like traditional energy. So, it has the potential to develop into a stable, light weight, and sustainable new energy source to power the electronic devices of the IoT era.

The triboelectric nanogenerator (TENG) has been proved to be a revolutionary energy harvesting technology since it was first proposed by Wang et al. in 2012 [26]. In daily life, triboelectric effect is usually considered as a harmful physical phenomenon which could cause the damage of electronic equipment. It is mainly caused by the transfer of electrons formed by the contact of two different substances. Wang et al. creatively took advantage of this phenomenon to convert mechanical energy into electrical energy. TENG generates potential difference through the relative motion of two kinds of friction materials with different electrostatic sequences, driving the internal and external carriers to supply power to the load. Compared to other energy collection technology, TENG has advantages of clean, high output performance, light weight, low cost, simple design and fabrication and wearable, implantable compatibility, etc. [6, 27, 28].

Address correspondence to Juan Wen, wenj@lzu.edu.cn; Yong Qin, qinyong@lzu.edu.cn

TENG has been considered as one of the most potential alternative energy sources for IoT devices [29, 30], but in previous researches, the performance of TENG was generally measured by indexes of open circuit voltage and short-circuit current, which can not completely reflect the performance of TENG as power source. For example, when the TENG with large open circuit voltage and short-circuit current supplies power to the sensor, the output power of the TENG is small because the inherent capacitance of the triboelectric nanogenerator is large and the resistance of the sensor is small. Only when the load resistance is equal to the internal resistance of TENG, the output power of TENG reaches the maximum. In addition, even if the output power of TENG is large enough to power the electrical equipment, it may not be directly used because the output waveform is too chaotic. In summary, TENG's output is characterized by high voltage and low current due to the presence of inherent capacitance, resulting in small actual output electricity on the load. At the same time, the charge density is limited due to the air breakdown phenomenon. In addition, due to the TENG operation mechanism and instability of environmental mechanical energy, the output signal of TENG is generally unstable, unpredictable, and presenting alternating current (AC) characteristics. All these have affected the output performance of TENG, and thus affect the practical application of TENG. Therefore, we described TENG's performance more systematically from a new perspective of powering ability, that is, the ability to output high quality electricity to the load efficiently as a power source. It consists of two aspects: the ability to transport charge effectively and the ability to output high power quality current steadily.

Fortunately, the output signal's management strategies aimed at promoting TENG powering ability have gained great attention from researchers in recent years. Different from general material selection, surface modification and structural design, the output signal's management strategies are to improve the intrinsic output performance of TENG and set up a suitable power management circuit (PMC) to improve the powering ability, so as to promote the development and application of TENG. The research on the output signal's management strategies can be mainly divided into four broad categories: improving the cycle output electricity of TENG, increasing the surface charge density of TENG, improving the power quality of TENG-based energy harvesting system, and promoting the application of TENG through IC technology and TENG network. Firstly, in order to improve the cycle output electricity of TENG, a mechanical switch [31] or a self-powered switch [32, 33] has been proposed to design the working cycle of the maximum output electricity of TENG. Secondly, the surface charge density of TENG directly affects the output voltage, current density, and power density of TENG [34]. Unfortunately, it is severely restricted by the phenomenon of air breakdown [35]. To overcome this problem, some works have introduced the charge pump structure which greatly improves the surface charge density and the output performance of TENG [35–37]. Thirdly, for the sake of improving the power quality of the power supply under a specific load and obtaining a high-power quality source with stable available direct current (DC) output, AC/DC conversion circuit, direct current triboelectric nanogenerator (DC-TENG), and impedance conversion circuit have also been widely used [36, 38–45]. Finally, in order to improve the technology maturity and universality and promote the application of TENG, the integrated output signal management module including IC technology and TENG network has been widely used [46, 47]. Through these output signal's management strategies, the power supply capacity of TENG is effectively improved, and the practicability of TENG-based energy harvesting system as a basic power supply unit is improved. The overview of the output signal's management strategies is shown in Fig. 1.

The output signal's management strategies are great significance for improving the powering ability of TENG. In order to build a practical TENG-based energy harvesting system, it is necessary to systematically summarize the development status and progress of these output signal's management strategies. In this review, we will firstly discuss the powering characteristics of TENG, including the electrical characteristics of TENG itself and the powering characteristics under different loads. After that, we will introduce the latest development of TENG output signal's management strategies and their contribution to improving the powering ability of TENG from the following four aspects: improving the cycle output electricity of TENG, increasing the surface charge density of TENG, improving the power quality of TENG-based energy harvesting system, and promoting the application of TENG through IC technology and TENG network. Finally, we summarize the existing challenges and trends, and prospect the possible development direction of the output signal's management strategies on TENG in the future.

2 The powering characteristics of TENG

To avoid the damage to the TENG output caused by improper circuit design, a thorough understanding of the TENG is particularly necessary. In this section, we will first analyze the electrical properties of TENG. After that, we will analyze the resistive load characteristics, capacitive load characteristics, and battery charging process of TENG. Based on above theoretical analysis, we can better comprehend the function of the output signal's management strategies.

2.1 Electrical properties of TENG

TENG utilizes the surface electrostatic charge generated by the contact of two different materials and the electric field that changes with time to drive the flow of electrons in the external circuit. Since it was first proposed in 2012, TENG has developed four main modes of work: vertical contact-separation mode [48], in-plane sliding mode [49], single electrode mode [50], and free-standing mode [51]. In recent years, Wang has proved that Maxwell's displacement current is the theoretical source of the nanogenerators [52, 53]. By introducing in electric displacement D, an additional term P_s that represents the polarization generated by electrostatic surface charges, the displacement current density can be obtained by

$$J_D = \frac{\partial D}{\partial t} = \varepsilon \frac{\partial E}{\partial t} + \frac{\partial P_s}{\partial t} \quad (1)$$

The second additional term $\partial P_s/\partial t$ is the current caused by the polarization field of the electrostatic charge carried by the surface, which is the theoretical basis and source of nanogenerators. The working mechanisms of TENG based on displacement current interpretation is shown in the Fig. 2(a). With the Maxwell's displacement current theory, the output characteristics of TENG based on internal current can be derived, which lays a theoretical foundation for the following capacitance model theory.

Before the theoretical models of Maxwell's displacement current equations were proposed, the traditional parallel plate capacitor (CA) model was the mainly used in most of the previous published researches [48–51, 54–57]. Different from the Maxwell's equations, the CA models obtain the dynamic transport process according to Ohm's law derived from the external circuit under the condition of load. It can also be said that CA model is a representation of displacement current output. Because it is built from the circuit theory, the CA models can provide useful guidelines for the design of output signal's management strategies as well as their practical applications. In the CA models, the most

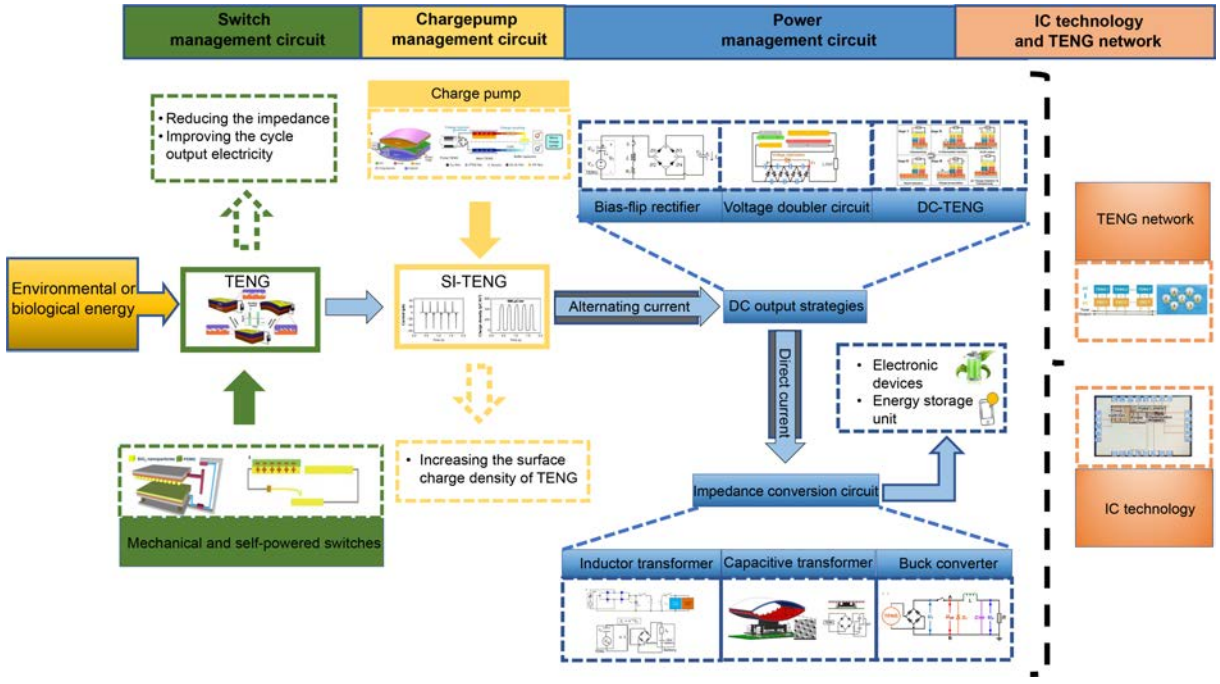

Figure 1 Overview of the output signal's management strategies. Reproduced with permission from Ref. [26], © Elsevier Ltd. 2012; Ref. [31], © American Chemical Society 2013; Ref. [33], © Elsevier Ltd. 2019; Ref. [35], © Cheng, L. et al. 2018; Ref. [36], © Liu, W. L. et al. 2019; Ref. [37], © Elsevier Ltd. 2018; Ref. [40], © Pu, X. et al. 2015; Ref. [41], © IOP Publishing Ltd. 2014; Ref. [42], © Elsevier Ltd. 2017; Ref. [43], © Wiley-VCH GmbH 2022; Ref. [44], © Pathak, M. et al. 2021; Ref. [45], © Niu, S. et al. 2015; Ref. [46], © Elsevier Ltd. 2019; Ref. [47], © Wiley-VCH GmbH 2020.

important thing is to get the relationship among three parameters: 1) its output voltage (V), 2) the amount of charge transferred between electrodes (Q), and 3) the separation distance (x) (V–Q–x relationship) [48, 49]. The TENG can be equivalent to a serial connection of an ideal voltage source and a capacitor, and the equivalent circuit model of a TENG is shown in Fig. 2(b) [55]. Hence, the governing differential equation can be given by

$$V = -\frac{1}{C(x)}Q + V_{oc}(x) \tag{2}$$

From Eq. (2), there are two main components that contribute to the total potential difference between the two electrodes. One part is from the polarized friction charge, that is $V_{oc}(x)$, which is the function of separation distance. Meanwhile, the charge transferred between electrodes (Q) also contributes. V–Q–x relationship is the governing equation of any TENG in the CA models, which clearly explains the intrinsic capacitance properties of TENG.

2.2 Resistive load powering characteristics

When a TENG directly connects to a resistive load without passing through the rectifier bridge, the equivalent circuit is shown in Fig. 2(c) [58]. And the governing equation can be given as

$$R\frac{dQ}{dt} = -\frac{Q}{c} + V_{oc} \tag{3}$$

Because the exist of the internal capacitance impedance of TENG, the load resistance has a significant effect on the instantaneous power output. The influence of the load resistance on the instantaneous power output is shown in Fig. 2(c). As we can see, the instantaneous output power increases first and decreases with the increase of load resistance later. In fact, above output characteristic can be explained by the impedance matching between the intrinsic capacitance of the TENG and the resistive load. When the load impedance is less than 1 kΩ, the total impedance is mainly determined by the intrinsic capacitance impedance of the TENG, so that the current remains almost constant. Then, when the load resistance matches the TENG's impedance (~ 100 MΩ) [48, 50, 51], the maximum output power of the TENG can be achieved. And when the load resistance is greater than 1 GΩ, the TENG almost works in the open circuit state, so the output power is reduced.

As can be seen from the above analysis, due to its inherent capacitance, TENG is unable to effectively power an impedance load with low resistance value, which could cause great energy loss.

2.3 Capacitive load powering characteristics

Capacitive load is another very important load case for TENG. When a contact-separation mode TENG charges the capacitive load (C_L) in the case of unidirectional motion, its equivalent circuit model is shown in the Fig. 2(d) [54]. When the motion of the dielectric layer reaches the maximum separation distance, the total stored energy in the capacitor (E_C) can be given by

$$E_C = \frac{C_L[Q_{SC}(x = x_{max})]^2}{2(C_L + C_T)^2} \tag{4}$$

It can be deduced from the above equation that when C_L is equal to the intrinsic capacitance (C_T) of TENG, the load capacitor can store maximum energy. The influence of the load capacitor on the total stored energy in the C_L is shown as Fig. 2(d), which could prove this inference. Hence, the load capacitor also has a conspicuous effect on the total stored energy. Considering that in real life situations, the intrinsic capacitance of the TENG is very small (usually in nano farad level) while the storage capacity is generally large (larger than microfarad level), it is also inefficient to use the TENG directly to power the capacitor directly.

2.4 Battery charging characteristics

In practice, TENG is basically driven by periodic mechanical motions. Therefore, it is necessary to use a full wave rectifier (FWR) to provide DC to the load. In this section, we will illustrate the charging characteristics of TENG in periodic mechanical motions with the battery as the load [44].

The equivalent circuit of the TENG charging the battery load through a rectifier bridge under periodic mechanical motion is

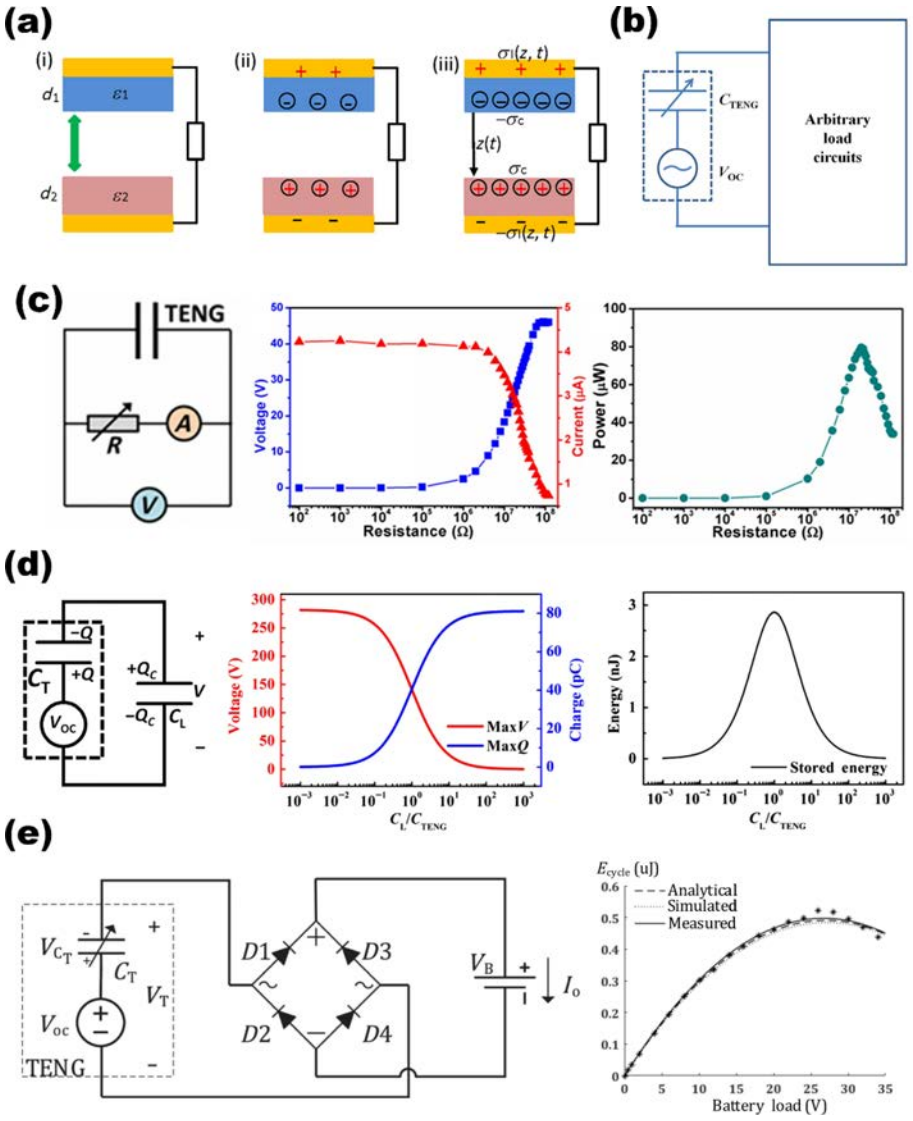

Figure 2 The Powering characteristics of TENG. (a) Working mechanisms [52] and (b) equivalent circuit model [55] of TENG based on Maxwell displacement current. Reproduced with permission from Ref. [52], © Wang, Z. L. 2016; Ref. [55], © Elsevier Ltd. 2014. (c) Equivalent circuit model of the whole TENG system when TENG is connected with resistance loads, and the influence of the load resistance on the magnitude of the output current, voltage, and instantaneous power output. Reproduced with permission from Ref. [58], © Elsevier Ltd. 2018. (d) Equivalent circuit model of the whole TENG system when TENG is connected with capacitance loads, and the influence of the load capacitance on the final voltage, charge stored in the load capacitor and final stored energy. Reproduced with permission from Ref. [54], © Elsevier Ltd. 2014. (e) Circuit scheme of TENG charging battery through rectifier bridge, and the analytical, simulated, and measured per-cycle energy plots against the battery load for FWR. Reproduced with permission from Ref. [44], © Pathak, M. et al. 2021.

shown in the Fig. 2(e). Because the diode has a voltage drop (V_D) and the battery's own voltage (V_B), the battery charging begins at the time when the TENG open circuit voltage ($V_{OC}(t)$) exceeds the sum of the battery voltage and the diode voltage drop ($V_B + 2V_D$). By mathematical calculation, the per-cycle energy output E_{cycle} can be given by

$$E_{cycle} = 2V_B C_{T,min}\left[V_{OC,max} - (1+\beta)(V_B + 2V_D)\right] \quad (5)$$

where $V_{OC,max}$ is the maximum open circuit voltage between two plates; $C_{T,min}$ is the minimum capacitances, β is the ratio of the capacitances at the two extremes ($\beta = \frac{C_{T,max}}{C_{T,min}}$). By calculating the Eq. (5), the optimal battery load (V_B^*) can also be given by

$$V_B^* = \frac{V_{OC,max}}{2(1+\beta)} - V_D \quad (6)$$

Based on above equations, through calculation, simulation, and experimental verification, the plot of per-cycle energy output relative to battery load can be obtained, as shown in Fig. 2(e). As illustrated, the maximum per-cycle output can be obtained when the battery load is 26.7 V, which is about 0.5 nJ.

3 Improving the cycle output electricity of TENG

The intrinsic impedance of TENG is large, but the electrical impedance of actual load is generally small, resulting in impedance mismatch. Therefore, there is a large loss of the collected charge during transmission, resulting in a very low output electricity per cycle for a TENG operating in continuous periodic mechanical motion. The output electricity per cycle of TENG can be calculated using the enclosed area of the closed loop in the V–Q plot [34]. Thus, improving the charging cycle to maximize energy-storage efficiency by modulating the charge flow with mechanical and self-powered switches is a feasible and reliable option [31–33, 59–62].

Cheng et al. presented an instantaneous discharging (ID) TENG controlled by a mechanical trigger switch [31]. As shown in Fig. 3(a), the charge generated by the TENG would be stored in the intrinsic capacitor and discharged outward only when the

switch is triggered. So that it can reach a relatively high output of 0.53 A and 142 W with a load of 500 Ω, which shows that the output impedance is significantly reduced. In fact, this result can be explained by the law of switching. At the moment, when the switch is closed, the internal capacitance of TENG is instantly equivalent to a constant voltage source. Its voltage does not change dramatically in that second, but the discharge time is greatly reduced. Therefore, the instantaneous output current is greatly improved without sacrificing the output voltage, as shown in the Fig. 3(b).

Further, *V*–*Q* plot was adopted to illustrate the step-by-step charging processes of both the direct and the designed charging cycles [59]. Due to the accumulated voltage on the capacitor, state of 0 and the maximum short-circuit transferred charge ($Q_{SC,\ max}$) in the *V*–*Q* plot is hard to reach, making the area of *V*–*Q* plot relatively small. While, this problem can be solved by use of switch control and the efficiency of charging is greatly improved. The improved charging cycle is shown as the Fig. 3(c). Thus, planning the charge–discharge cycle is highly advantageous for improving the charging rate, enhancing energy-storage efficiency (up to 50%), and promoting saturation voltage. This study has an important guiding significance for the use of the control switch.

Although motion trigger switches are easy to design and have been studied extensively, its application requires a special design of the structure of TENG, which makes the TENG system more complicated. In that case, they do not have a wide range of practicality. Recently, a type of universal self-powered switches without an external mechanical triggering has been proposed. As shown in Fig. 3(d), a self-powered air discharge switch that uses air breakdown is designed, whose on/off state is totally controlled by the voltage of the TENG itself [32]. By changing the tip-plate distance of the switch, the electric output of the TENG system can be easily modulated without excessive complicated structural design. Furthermore, it is found that the ultraviolet (UV) light can change the discharge mode of the switch and decrease the output current of the TENG, making it possible for that TENG system

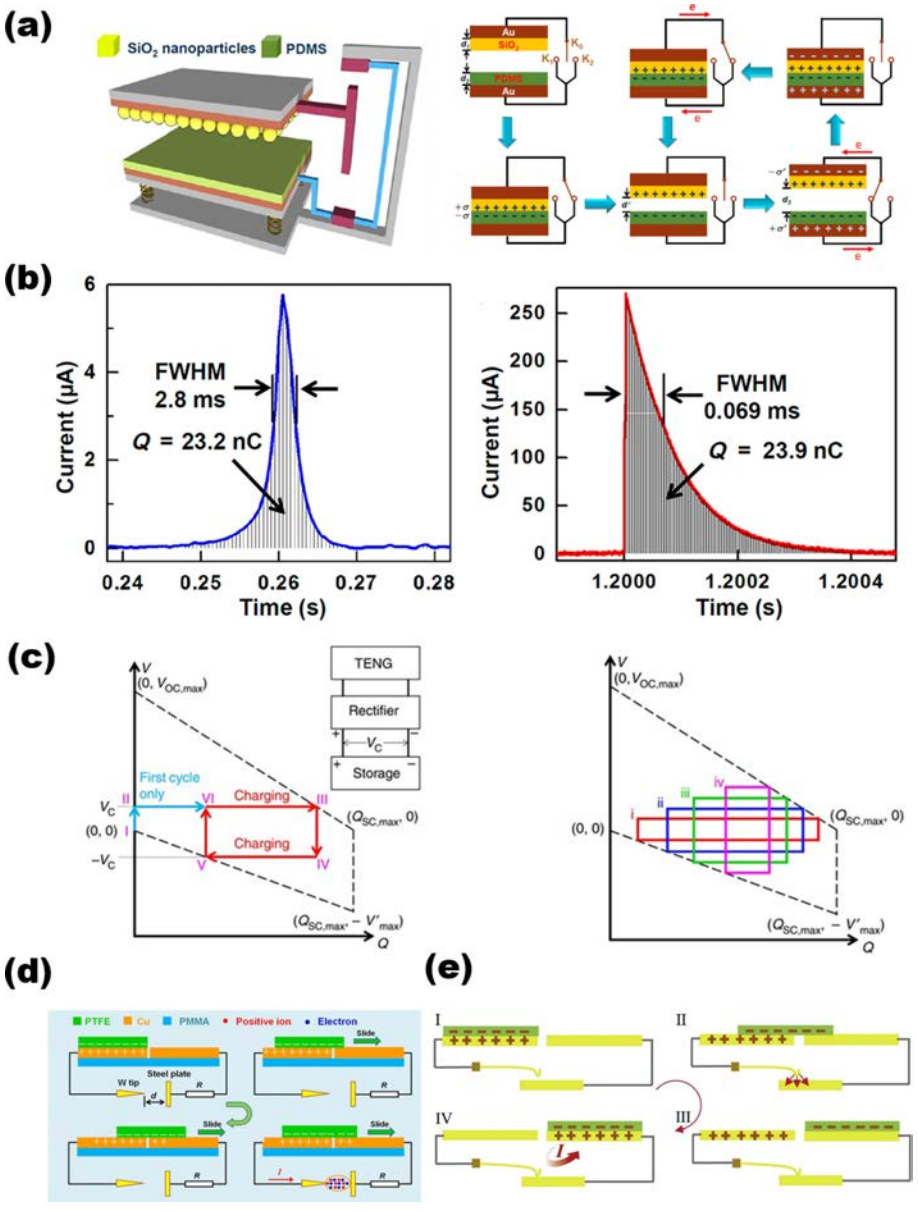

Figure 3 Improving the cycle output electricity of TENG. (a) Structure and working mechanism of discharging TENG. Reproduced with permission from Ref. [31], © American Chemical Society 2013. (b) Magnification of a single current peak of the normal TENG and instantaneous discharging TENG. Reproduced with permission from Ref. [31], © American Chemical Society 2013. (c) The V–Q plot of the circuit for the designed charging cycle and the designed charging cycle for different charging voltages. Reproduced with permission from Ref. [59], © Zi, Y. L. et al. 2016. (d) Working mechanism of the TENG with an electrostatic vibrator switch. Reproduced with permission from Ref. [32], © Elsevier Ltd. 2017. (e) Working mechanism of the Pulsed-TENG with an electrostatic vibration switch. Reproduced with permission from Ref. [33], © Elsevier Ltd. 2019.

with air discharge switch to be a self-powered ultraviolet sensor. Qin et al. further reduced the energy loss of the self-powered switch through developing electrostatic vibration switch, which could reach the energy storage efficiency of 57.8%, as shown in Fig. 3(e) [33]. The vibration frequency of the mechanical switch can be adjusted to match the operating frequency of the TENG, which could minimize the energy loss of the switch and achieve the maximum cycle energy output. With extremely low impedance, simple structure, low cost, and high efficiency, the self-powered switches are supposed to be a promising energy transfer management strategy and have promising applications in AC pulse source or forming a high-performance TENG-based energy harvesting system by combining with the subsequent circuit.

4 Increasing the surface charge density of TENG

Charge density is one of the important parameters of TENG, which determines the output voltage, current density, power density, and energy storing speed of TENG [34, 35]. Aiming at increasing the surface charge density of TENGs, previous works mainly focused on the selection of friction materials, surface treatment, and charge injection. However, air breakdown caused by the generated electric field heavily limits the increase of charge density, which cannot be solved by any of the above methods. The charge pump mechanism is an effective means to solve this problem [35, 37, 63].

Cheng et al. presented a self-improving triboelectric (SI-TENG) nanogenerator with improved charge density [35]. As shown in Fig. 4(a), the SI-TENG is divided into two parts. Part I is a TENG working in vertical contact-separation mode as the voltage source, while Part II is the inner plane-parallel capacitor structure (PPCS), which consists of two polyethylene terephthalate (PET) films with two electrodes insulated by polyvinylidene fluoride (PVDF)/epoxy resin (EP) films on each film. Part I generates a large amount of charge driven by the external vibration and enters the PPCS through a full wave rectifier. The generated charge would be stored in the PPCS with a high charge density and released to the subsequent circuit when driven by vibration. Through this design, the problem that charge density of TENG is limited by air breakdown is solved, and the output current and effective charge density are increased to 10.32 and 7.22 times that of part I as well as the maximum effective charge density is promoted to 490 μC/m^2. On this basis, Xu et al. put forward a self-charge-pumping TENG (SCP-TENG) combining floating layer structure and charge pump [37], as shown in Fig. 4(b). The SCP-TENG is composed of a pump TENG and a main TENG. The floating layer of the main TENG consists of a metal layer separated by two dielectric layers that can bind electric charges to the metal layer. Therefore, in practical applications, the floating layer continuously receives electrons from the pump TENG. These electrons accumulate and are bound in the floating layer, resulting in a high charge density and strong electric field in the main TENG. Finally, the SCP-TENG achieved an extremely high surface effective charge density of 1020 μC/m^2, four times that of air breakdown.

Furthermore, a high-performance triboelectric nanogenerator based on innovative charge shuttling mechanism (CS-TENG) was developed, as shown in Fig. 4(c) [63]. The CS-TENG is mainly composed of a pump TENG, a main TENG, and a buffer capacitor. Different from the ordinary charge pump mechanism, the CS-TENG traps the charge completely to the dielectric surface and supplies power for load by shuttling of the charge carriers between the main TENG and buffer capacitor. After the pump TENG has injected the charge into the main TENG, the capacitance of the main capacitor would vary with contacts and separations, while the capacitance of the buffer capacitor remains constant. In that way, the CS-TENG can generate the electromotive force that drives the charge shuttling on both sides between the main TENG and buffer capacitor, thus obtaining an ultrahigh charge density of 1.85 mC/m^2. Additionally, a wave energy harvesting device based on the CS-TENG is designed to verify the feasibility of the proposed mechanism and obtains a good operation effect. It shows that the charge pump mechanism can greatly increase the energy output by improving the design of the internal charge path of traditional TENG.

5 Improving the power quality of TENG-based energy harvesting system

The output signal of TENG is generally an unstable AC signal with high voltage and low current, which is generally considered as a low power quality power source and can not be used by electronic devices and charge energy storage unit directly. Fortunately, the AC/DC conversion circuit and the DC-TENG can convert the pulsed AC signal of TENG into a DC signal with the lowest possible energy consumption. Common AC/DC conversion circuits are full wave rectifier circuit, bias flip rectifier, and voltage multiplier circuit [64]. The impedance conversion circuit can reduce the output impedance of the energy harvesting system based on TENG and obtain the output signal of low voltage and high current. These two strategies are very important for the energy output management of TENG, which can significantly improve the power quality of TENG-based energy harvesting systems. In this section, we will briefly introduce each category.

5.1 The strategies of TENG's direct current output

At present, most electronic devices and charge energy storage units need DC for power supply. In order to convert the AC pulse signal generated by TENG into DC signal, the AC/DC conversion circuit is extremely necessary. The FWR is one of the most common AC/DC conversion circuits with advantages of simple design, high reliability, and ease of use. Based on unidirectional conductivity of diodes, it can convert AC signal to DC signal effectively. In Section 2, we have analyzed some of the transmission characteristics of the FWR. However, despite all the advantages mentioned of FWR, it has been demonstrated that some newly developed AC/DC conversion circuits can achieve higher per-cycle energy output, such as bias-flip rectifier and voltage doubler circuit. These recently proposed AC/DC conversion circuits have shown a promising development prospect and attracted researchers' attention.

The bias-flip rectifier, also known as parallel synchronized switch harvesting on inductor (p-SSHI), was firstly proposed by Guyomar et al. to apply to harvest piezoelectric energy [65]. The p-SSHI technology uses inductive capacitor resonant circuit to flip the voltage when the equivalent current of the piezoelectric sensor changes the direction at the peak point. In this way, the voltage at both ends of the piezoelectric sensor can be increased and the process of voltage direction reversal can be accelerated, so as the charge transfer efficiency is greatly promoted. Madhav and many other workers have conducted detailed analysis and comparison of energy loss between FWR and p-SSHI rectifiers [44, 66, 67]. As shown in Figs. 5(a) and 5(b), the energy loss of the p-SSHI system is much lower than that of the FWR system during the charge discharge cycle. It reveals that p-SSHI greatly reduces the charge loss in the conversion process. Khushboo et al. proposed to develop the AC/DC conversion circuit for TENGs based on the p-SSHI technique [68]. Figure 5(c) shows the circuit scheme of the standard interface circuit and the proposed p-SSHI AC/DC conversion circuit based on this. A typical SSHI circuit is modeled

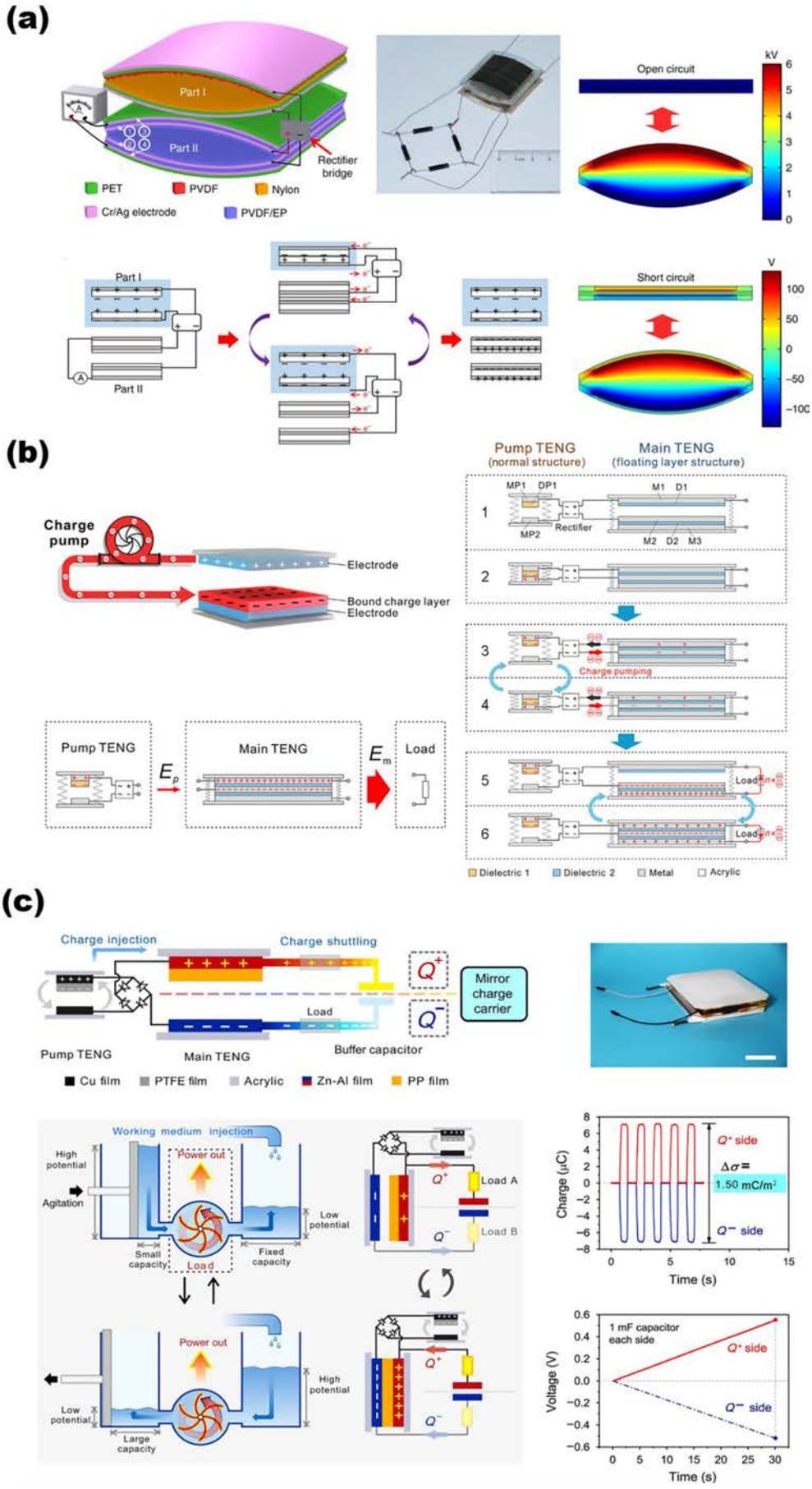

Figure 4 Charge pump mechanism for TENG. (a) Design, structure, and working mechanism of the self-improving triboelectric nanogenerator. Reproduced with permission from Ref. [35], © Cheng L. et al. 2018. (b) Device structure and working principle of the self-charge-pumping triboelectric nanogenerator. Reproduced with permission from Ref. [37], © Elsevier Ltd. 2018. (c) Device structure, working principle, and output charge density of the high-performance triboelectric nanogenerator based on charge shuttling. Reproduced with permission from Ref. [63], © Wang, H. M. et al.2020.

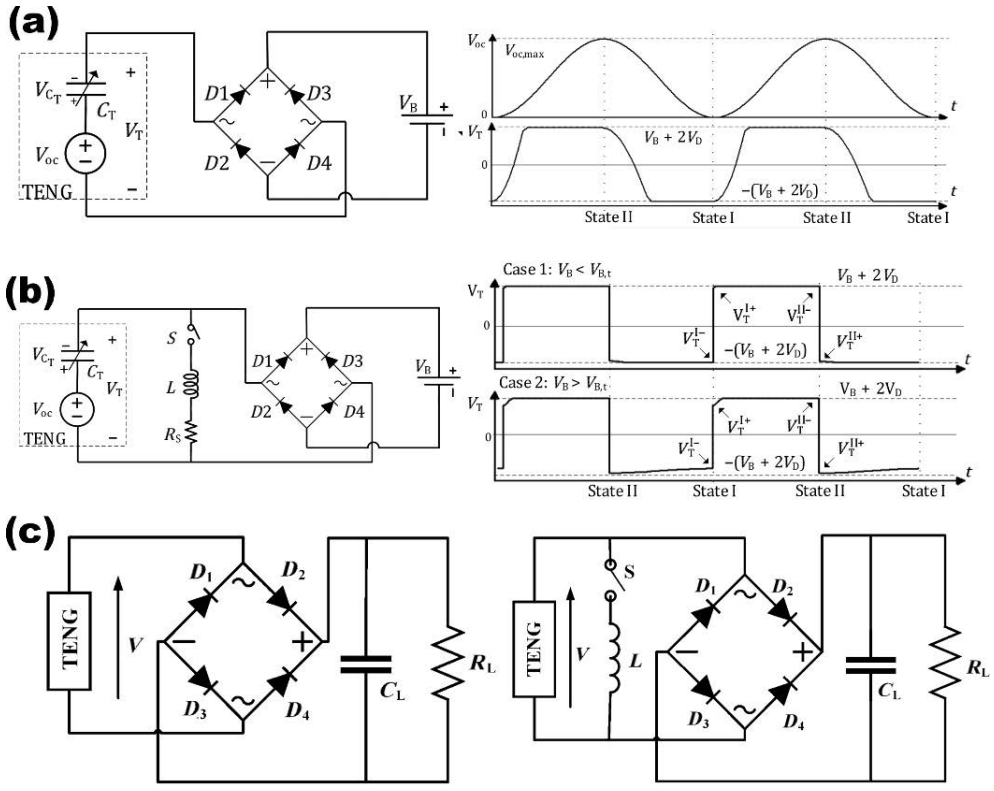

Figure 5 Switches circuit for the interface circuits of TENG. (a) Circuit scheme and voltage waveforms before and after rectification of full wave rectifier circuit. Reproduced with permission from Ref. [44], © Pathak, M. et al. 2021. (b) Circuit scheme and voltage waveforms before and after rectification of p-SSHI circuit. Reproduced with permission from Ref. [44], © Pathak, M. et al. 2021. (c) Scheme of the standard interface circuit and p-SSHI interface circuit. Reproduced with permission from Ref. [68], © The Minerals, Metals & Materials Society 2020.

as a power boosting circuit performing AC-to-DC rectification at optimum load resistance. Switch S is triggered to conduct for a short period of time under maximum and minimum mechanical displacement, maintaining the output voltage and current in the same phase, thereby not providing a return path for energy. The switching closing period of LC oscillation is set to be shorter than the mechanical vibration period, thus frequently keeping the TENG in the open configuration. However, the control switch connected in series with the inductor would consume a mass of energy. Hence, it is necessary to develop low power control switch circuit for p-SSHI circuit. The ZCD circuit can detect the zero-crossings of the inductor through monitoring the peaks of voltage across the harvester legs, thereby generating appropriate control signals [69].

Besides, voltage doubler circuit was also applicated as the AC/DC conversion circuit for environmental energy harvesting [36, 39, 70–75]. In the presence of diode non-idealities, the voltage doubler gives an improvement in the overall power obtained. More recently, the Bennet's doubler was also proved to be an effectively AC/DC conversion circuit for TENG [39, 73–75]. Inspired by the principles of Bennet's doubler device proposed in 1787, Ghaffarinejad et al. firstly proposed applying the Bennet's doubler conditioning circuit to the TENG [39, 73]. The circuit structure of Bennet's doubler conditioning circuit is shown in Fig. 6(a). Without complicated control components, the Bennet's doubler conditioning circuit is merely composed of two capacitors and three diodes. Through using diodes to reconfigure the charge flow, the voltage of C_{res} would increase along with the raising of working cycles as same as the surrounding area of V–Q plot, as shown in Fig. 6(a). Through theoretical analysis and experimental verification, it is proved that Bennet's doubler could increase the voltage on the capacitor to 835 V after 140 s, giving it a much stronger energy transfer capacity compared to half-wave and full wave rectifier [73]. Moreover, through a sequence of operations with four electrodes and the controlling of three switches, a programmed-triboelectric nanogenerator with a Bennet's doubler can achieve a ~ kV level voltage output without any material optimization [74]. The schematic diagram and structure of the Bennet's doubler based on programmed-triboelectric nanogenerators is illustrated in Fig. 6(b).

Additionally, voltage rectification circuit with higher magnification was also applicated in the circuit of interface circuit of nanogenerator. Liu et al. used a sixfold voltage-multiplying circuit as an interface circuit between the external TENG and the main TENG of the designed ECE-TENG [36]. As shown in Fig. 6(c), the voltage-multiplying circuit mainly consists of seven rectifier diodes and seven ceramic capacitors. In the case of AC power input, the rectifier diodes could control the direction of charge flow. This allows the ceramic capacitors to be charged during the positive half cycle and then be connected in series with power supply. As a result, the voltage could be boosted to six times the initial voltage after few working cycles. The designed voltage-multiplying circuit can be applied in the completed external and self-charge excitation modes.

In recent years, DC triboelectric nanogenerators that can directly convert mechanical energy into DC energy have entered people's vision. Wang et al. reported a cylindrical multiphase DC-TENG composed of three TENGs with different phases, as shown in Fig. 7(a) [76]. Due to the different initial positions of the Cu electrodes, the pulse signals generated by the three TENGs have different phases. A constant DC signal with a low peak factor of 1.08 can be obtained by phase coupling. In addition, Liu et al. developed insulator-based DC-TENG by contact electrification and dielectric breakdown, as shown in Fig. 7(b) [77]. When the friction electrode (FE) slides on polytetrafluoroethylene (PTFE), PTFE and FE are negatively and positively charged, respectively, and an electric field is generated between charge collecting electrode (CCE) and PTFE. When the electric field is large

enough, the electrons on the surface of PTFE are transmitted to CCE under the action of air breakdown, and then transferred to FE through an external circuit, finally generating a DC signal. On this basis, as shown in Fig. 7(c), Zhao et al. realized the miniaturization of the slider structure and the high charge density of DC-TENG through microstructure design [78]. In order to further reduce the energy loss and improve the output stability, Li et al. designed a constant voltage DC-TENG (C-DC-TENG) with stable output performance by using the ternary dielectric triboelectrification effect, as shown in Fig. 7(d) [43]. The C-DC-TENG fabricated by introducing polyester fur as the third tribo-layer into the traditional binary grating structure TENG has high output power and extremely low crest factor of 1.0082.

5.2 Reducing the output impedance of TENG-based energy harvesting system

After the interface circuit conversion, the output signal of TENG has changed into DC signal, but it still has the characteristics of high-voltage and low-current. Therefore, in order to obtain a stable low voltage current, further impedance conversion is necessary. Below we will introduce several different impedance conversion circuits, including capacitive transformer, inductor transformer as well as buck converter.

In previous works of impedance conversion circuits, energy storage elements such as inductor and capacitor are generally applied. Among them, the inductive transformer is the most common and simple structure strategies [40, 45, 79–82]. Wang et

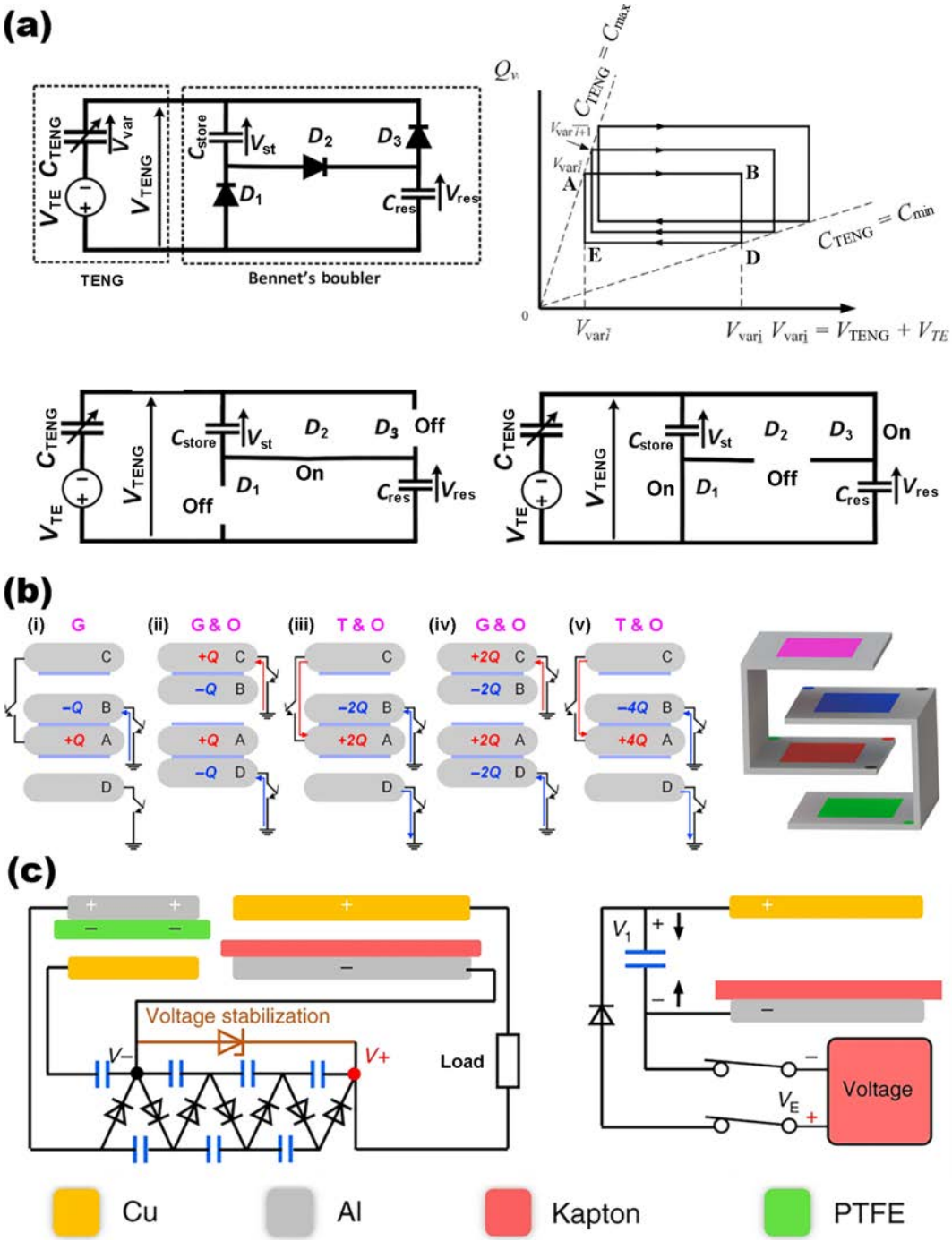

Figure 6 Voltage doubler circuit for the interface circuits of TENG. (a) Scheme, working mechanism and the *V*–*Q* plot in steady-state of Bennet's doubler circuit. Reproduced with permission from Ref. [73], © Elsevier Ltd. 2018. (b) Working mechanism and structure of the proposed programmed-triboelectric nanogenerators for realizing Bennet's doubler. Reproduced with permission from Ref. [74], © Elsevier Ltd. 2020. (c) Systematical electric circuit and simplified working components of the external charge excitation TENG. Reproduced with permission from Ref. [36], © Liu, W. L. et al. 2019.

al. proposed a power management circuit composed of a spark switch and a matching inductance transformer [82]. As shown in Fig. 8(a), an ultra-high voltage (over 7.5 kV) energy management system has been established for TENG through an inductive transformer. The converted DC output can drive the sensor network and power commercial LEDs. Pu et al. researched the coil ratio of the inductor transformer [40]. It found that the highest charging efficiency of 72.4% could be achieved at the coil ratio of 36.7 and the matching impedance can be reduced to 110 Ω, as shown in Fig. 8(b). However, because of the inherent characteristics of inductor transformer, only when TENGs work near the central frequency of the inductor transformer can the higher energy transfer efficiency be obtained. Thus, Niu et al. presented a different buck converting strategy using inductor with two active switches included [45]. Figure 8(c) reveals the electric circuit scheme of the proposed design. TENG charged the C_{temp} through a full wave rectifier firstly, then the switches J_1 and J_2 would close in sequence to ensure that the charge could be effectively transferred from the C_{temp} to the final energy storage unit through the coupled inductor. In that way, it realized the conversion efficiency of 59.8% from the AC output produced by TENG to DC output port and can be running at a low working frequency.

Compared to the inductance transformer which relies on the principle of electromagnetic induction work, capacitive transformer realizes the buck converting mainly by changing the series and parallel state of capacitor array [41, 83, 84]. Tang et al. proposed a power-transformed-and-managed triboelectric nanogenerator (PTM-TENG), in which capacitive transformer could be automatically triggered by motion of the PTM-TENG, and achieved a high energy preservation efficiency and low output impedance at a low operating frequency [41]. Schematic and working principle of the PTM-TENG is shown in Fig. 9(a). On the basis of results above, Liu et al. proposed a fractal-design-based switched-capacitor converter (FSCC), as shown in Fig. 9(b) [84]. The FSCC contains a fixed number (N) of capacitors, which could be controlled by a single-pole double-throw switch to transform between series and parallel state. Regardless of the loss of the diode, when N capacitors are charged in series and then switched to parallel to discharge, the output voltage would drop to a quarter of the voltage source while the output charge becomes four times of the input charge. The operating mechanism and circuit scheme of FSCC are shown in Fig. 9(c). Meanwhile, the FSCC is divided into different orders according to the different combinations of capacitors. Figure 9(c) shows the concept of fractal structure evolution in increasing order, along with a similar design based on fractal structure evolution for FSCC also arranged in increasing order [84]. The order of FSCC can be selected according to the amount of charge that needs to be converted, and multi-order FSCC was proved to have lower charging loss in diodes. Thus, with double-function output modes, FSCC achieved the advantages of minimum output impendence and high electrostatic voltage applicability, and was proved huge potential in TENG power management.

Buck converter topology is a kind of classical DC/DC conversion circuit. Controlled by certain duty cycle switching waveform, it can generate stable DC current which voltage is lower than input energy source [33, 42, 46, 66, 69, 85–90]. The idea of using buck converter for power management for weak mechanical energy collection is shown in Fig. 10(a) [90]. In recent years, Xi et al. reported a novel power management circuit based on buck converter [42]. As shown in Figs. 10(b) and 10(c), the buck converter is controlled by a switch consisted of a micro-power voltage comparator and a MOSFET. Switch can autonomously turn on when the voltage of TENG reaches to the peak so that the harvested energy can be transferred to the LC unit. Then, the energy stored in the LC unit would be released to the load smoothly. However, the drive and control of MOSFET need corresponding driver and logic circuit, in that case the related circuit cannot work without a dedicated power supply. To solve that problem, Harmon et al. reported a fully functional buck converter system without any additional power supply [87]. As shown in Fig. 10(d), a silicon-controlled rectifier (SCR) and Zener diode were combined as switch to control the power flow paths without using any integrated circuit. Through this circuit, the proposed power management system greatly reduced the output impedance and achieved an overall energy conversion efficiency of 84.3%, as illustrated in Fig. 10(d). Compared to inductor and capacitive transformers, buck converter can work over all frequency ranges and does not require external power supply to drive the control elements, which makes it to be a broad energy management strategy for TENGs potentially.

6 Promoting the application of TENG through IC technology and TENG network

Positive progress has been made in these TENG output signal's management strategies above, and the conversion efficiency is up to 84.6%, which makes it possible to effectively manage the charge generated from TENG in a variety of ways. However, most of these output signal's managements have low maturity and poor universality, so there are still difficulties in practical application of TENG system. Therefore, it is particularly necessary to develop integrated and real-time output signal's management modules, including the exploration of TENG network and IC technology. In this section, we will discuss the recent progress of application of TENG network and IC technology, as well as the potential applications enabled by integrating with TENG as a TENG-based energy harvesting system.

6.1 TENG network

At present, most of the research on output signal's management strategies are focused on a single TENG. However, the electricity provided by a single TENG is not enough to power larger electronic devices, so it is necessary to connect large TENG arrays via output signal's management strategies to better capture environmental energy. For the past few years, some useful explorations have been made in the application of TENG network. Liang et al. proposed a hexagonal TENG network with seven spherical TENG units linked by rigid strings, which was fabricated to harvest wave energy [47, 88, 91]. As shown in Fig. 11(a), charge excitation circuits (CEC) based on the voltage-multiplying circuit was firstly designed, which could increase the output performance of a single TENG by multiple times [47]. After that, each TENG unit of the TENG network was connected to a CEC respectively and then directly connected in parallel through the Output 1 of the CECs without rectified bridges. Integrated with the CECs, the proposed TENG network with output signal's management strategies obtained a maximum current of 24.5 mA and maximum power of 24.6 mW with the wave frequency of 0.6 Hz and the wave height of 10 cm. And it also has been shown to drive a thermometer continuously and realize the wireless communication between wireless transmitter and phone. There are also works that connect the TENG network with the reported output signal's management strategies, such as buck converter, to form a complete energy harvesting system. These efforts have achieved positive results, as shown in Fig. 11(b) [88]. Above work has proved that, due to the stack of multiple TENG, the stability of the waveform and the density of output current peaks are significantly improved. Additionally, the output matching

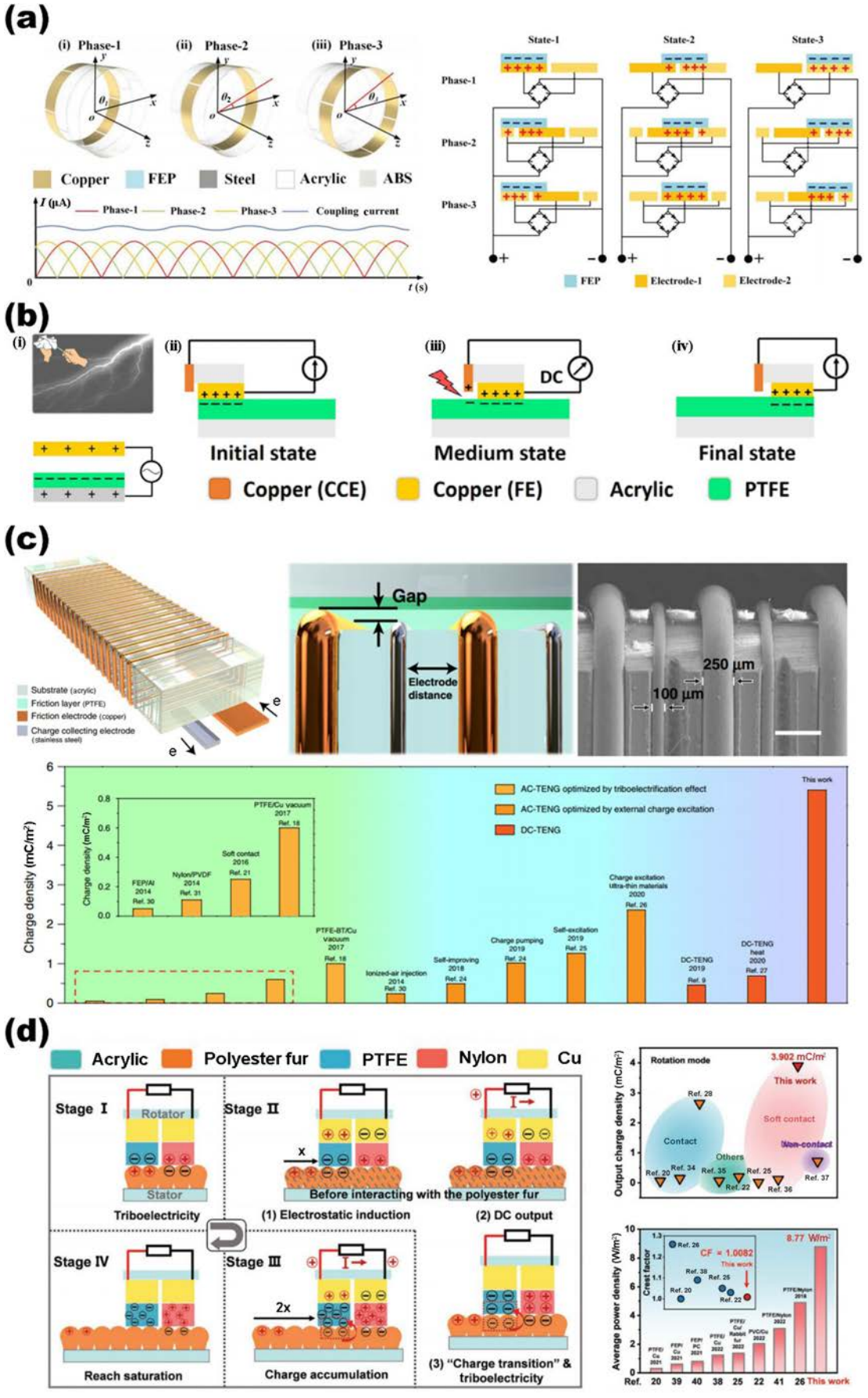

Figure 7 The structure and corresponding output performance of DC-TEGN. (a) The working principle diagram of Phase-coupled DC-TENG and the schematic diagram of each phase current at different times. Reproduced with permission from Ref. [76], © WILEY-VCH Verlag GmbH & Co. KGaA, Weinheim 2020. (b) The working principle of electrostatic breakdown DC-TENG. Reproduced with permission from Ref. [77], © Liu D. et al., some rights reserved; exclusive licensee American Association for the Advancement of Science 2019. (c) Structure design and charge density of MDC-TENG. Reproduced with permission from Ref. [78], © Zhao, Z. H. et al. 2020. (d) The working mechanism and output performance of C-DC-TENG before the dielectric layer reaches charge saturation state. Reproduced with permission from Ref. [43], © Wiley-VCH GmbH 2022.

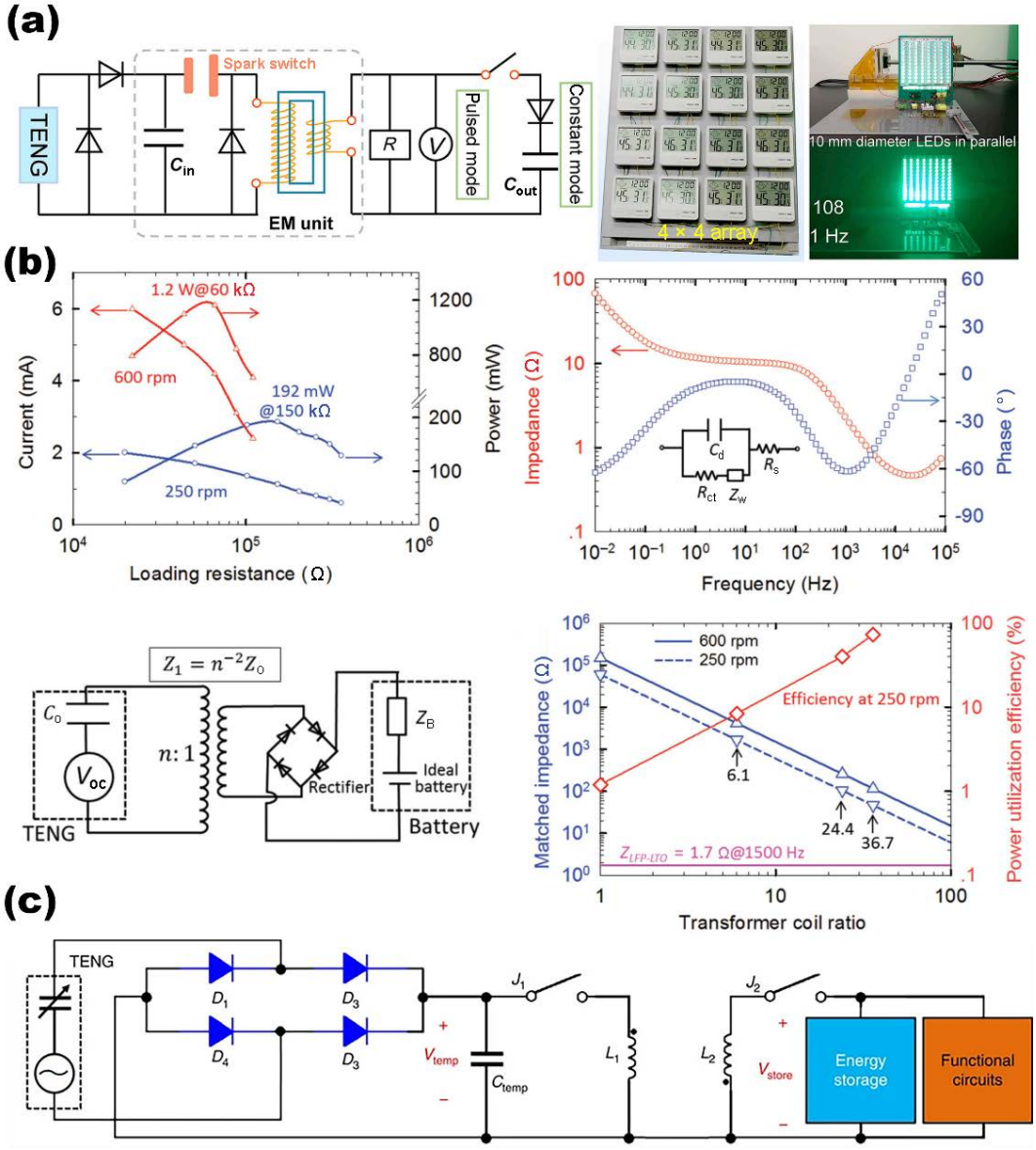

Figure 8 Inductor transformer for TENG. (a) Circuit scheme and application display of the inductor transformer for TENG. Reproduced with permission from Ref. [82], © Elsevier Inc. 2020. (b) The variation of TENG's current and power with external resistance, the Bode diagram of battery impedance, the equivalent circuit scheme of TENG charging battery through inductor transformer and the influence of transformer coil ratio on TENG matching impedance. Reproduced with permission from Ref. [40], © Pu, X. et al. 2015. (c) Circuit scheme of the proposed power management circuit with a coupled inductor. Reproduced with permission from Ref. [45], © Niu, S. et al. 2015.

resistance is significantly decreased due to the increase of the total capacitance, highlighting the advantages of TENG network over a single TENG. Furthermore the targeted development of output signal's management strategies is the key to better manage the energy of TENG network.

6.2 IC technology

All of the above output signal's management strategies can effectively reduce the charge loss in the transmission process, but these works generally have a single function and large size, which are difficult to adapt to diverse work requirements. In order to achieve modular, multi-functional, and miniaturization while minimizing charge loss, IC technology has been integrated into the research of output signal's management strategies [46, 67, 69, 85, 89, 92]. Yoo et al. designed a new boost-type DC-to-DC converter CMOS IC optimized for the TENG as shown in Fig. 12(a) [46]. It can generate reliable DC voltage under TENG's ranging output. And the optimum moment to transfer electrical energy into the electronic device is automatically traced by zero current switching and input voltage estimation to reduce the power consumption of the circuit evidently. In the automatic control of the moment when the electrical output of the TENG is transferred into the electronic device, the IC shows a conversion efficiency over 70% even when the input power is about 2.5 μW. In another work, a complete power management system was designed for TENG through IC technology. As shown in Fig. 12(b) [93], integrating the LTC3330 chip with TENG can convert the output signal of TENG into a signal suitable for most applications. The efficiency of this integrated circuit for high-voltage TENG can reach 78%, which can drive certain small electronic products and is widely used in environmental sensors and wearable personal electronic products. Those works verified the feasibility of IC technology in application of output signal's management strategies, and provided a promising strategy for the practical application of the TENG-based energy harvesting system. However, the control unit needs to further reduce power consumption to improve the end-to-end efficiency and the voltage bearing capacity of the input port also needs to be further improved through the improvement of circuit scheme.

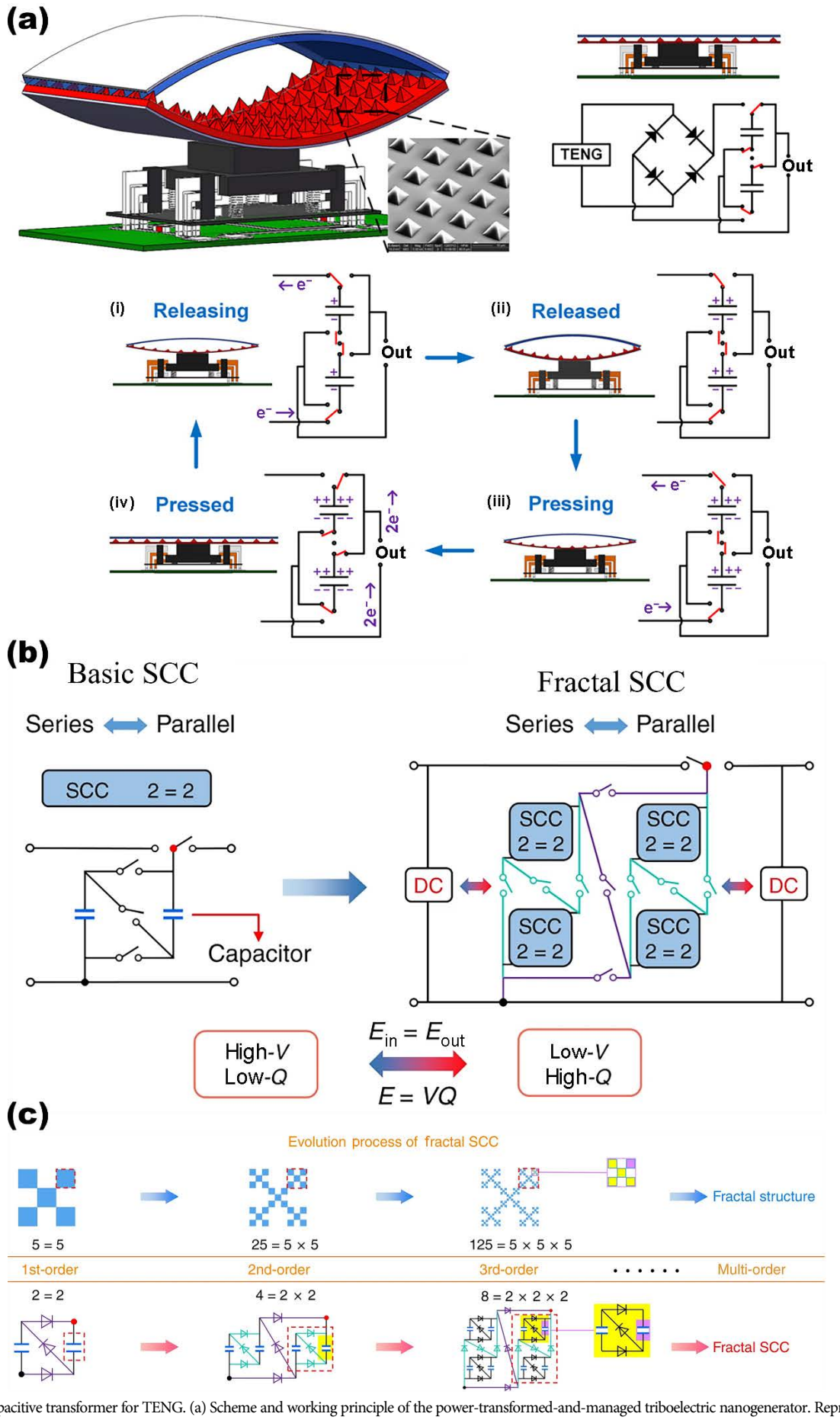

Figure 9 Capacitive transformer for TENG. (a) Scheme and working principle of the power-transformed-and-managed triboelectric nanogenerator. Reproduced with permission from Ref. [41], © IOP Publishing Ltd. 2014. (b) The operating mechanism of a conventional electromagnetic transformer, a basic switched- capacitor convertor and a fractal design based switched-capacitor-convertor. Reproduced with permission from Ref. [84], © Liu W. L. et al. 2020. (c) The evolution process of fractal design based switched-capacitor-convertor. Reproduced with permission from Ref. [84], © Liu, W. L. et al. 2020.

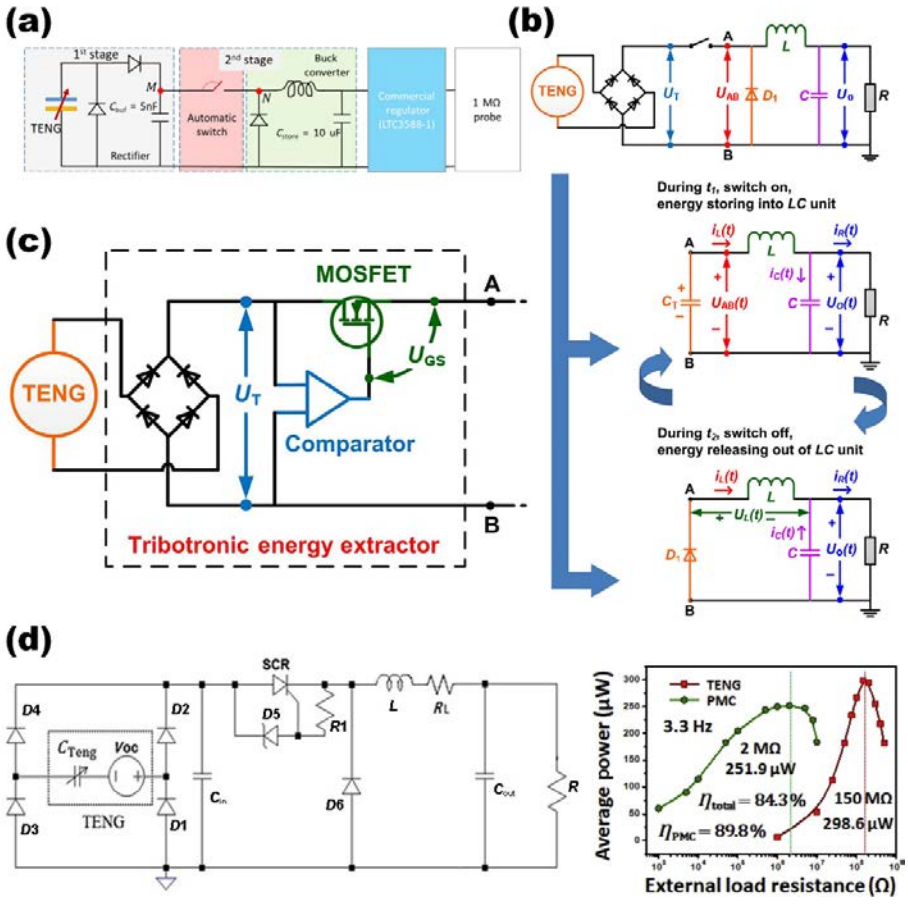

Figure 10 Buck converter for TENG. (a) Scheme of the proposed energy harvesting circuit with buck converter. Reproduced with permission from Ref. [90], © Zhang, H. et al. 2019. (b) The circuit scheme and working mechanism of AC-DC buck conversion by coupling TENG, rectifier and classical DC-DC buck converter. Reproduced with permission from Ref. [42], © Elsevier Ltd. 2017. (c) The schematic diagram of the tribological energy extractor (TEE) based on the Buck converter. Reproduced with permission from Ref. [42], © Elsevier Ltd. 2017. (d) Complete circuit scheme of the proposed power management circuit (PMC), the output power of TENG and PMC against load resistance, efficiency of PMS and overall conversion efficiency. Reproduced with permission from Ref. [87], © Elsevier Ltd. 2020.

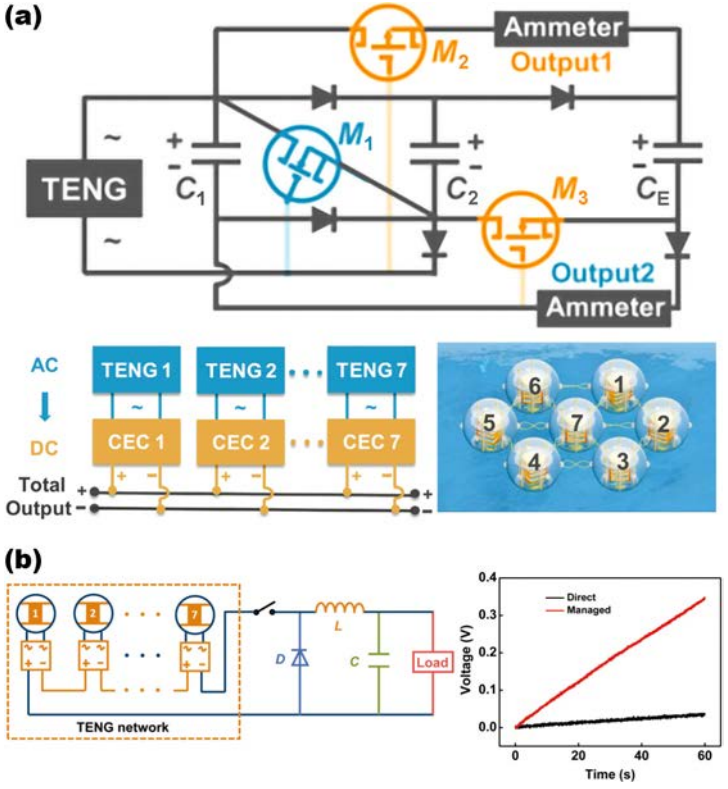

Figure 11 Application of TENG network. (a) Scheme of the charge excitation circuit (CEC) integrated with the TENG and sketch of the TENG network with CECs. Reproduced with permission from Ref. [47], © Wiley-VCH GmbH 2020. (b) The TENG network integrated with the buck converter and the comparison of the TENG network between the managed charging and direct charging for a 10 mF capacitor. Reproduced with permission from Ref. [88], © WILEY-VCH Verlag GmbH & Co. KGaA, Weinheim 2019.

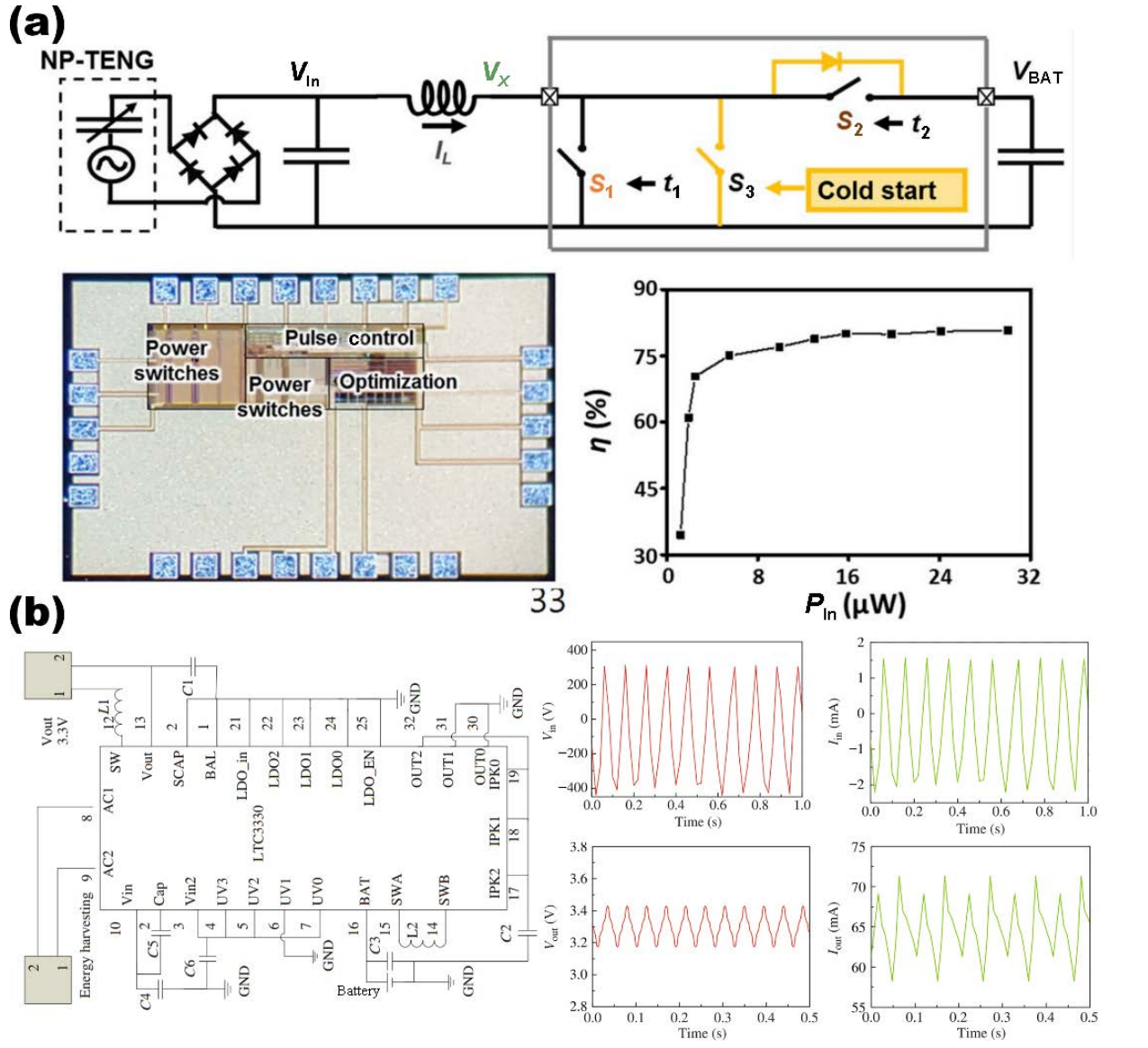

Figure 12 Application of IC technology for TENG. (a) Top layer architecture, chip micrograph and power conversion efficiency diagram of triboelectric energy collection system based on CMOS IC. Reproduced with permission from Ref. [46], © Elsevier Ltd. 2019. (b) Triboelectric energy collection system integrated with TENG and LTC3330 chip and its output performance. Reproduced with permission from Ref. [93], © Science China Press and Springer-Verlag Berlin Heidelberg 2016.

7 Summary and prospective

TENG-based energy harvesting system offers a promising solution to the long-term power supply problem of IoT devices. Enhanicng its powering ability is a very important topic. In this review, we systematically summarized how to enhance the powering ability of the TENG-based energy harvesting system through output signal's management strategies. Output signal's management strategies of TENG can be categorized into the mechanical and self-powered switches circuit, the charge bump circuit, the power management circuit, and IC technology and TENG network. These strategies serve different functions such as improving the cycle output electricity of TENG, increasing the surface charge density of TENG, improving the power quality of TENG-based energy harvesting system, and promoting the application of TENG through IC technology and TENG network. In order to increase the output electricity of TENG for each cycle, mechanical switches and self-powered switches are proposed to improve the energy transfer capacity of the charge generated from TENG. These switch management circuits greatly reduce the output impedance by improving the working cycle of TENG. Charge pump management circuits are widely used to improve the charge density of TENG, which can significantly increase the surface charge density through the use of internal capacitors, thus improving the output electricity of TENG. As for aspect of improving the power quality of TENG-based energy harvesting system, AC/DC conversion circuit, DC-TENG, and impedance conversion circuit are proposed in this paper, which can convert the pulse signal with high output impedance of TENG into DC signal with large current and low voltage. With the use of bias-flip rectifier and the voltage doubler circuit, the interface circuit can accomplish the AC/DC conversion more efficiently than the traditional FWR. In addition, DC-TENG can directly convert mechanical energy into DC energy and achieve different goals such as charging energy-storage capacitor and supply power for electronic devices. To further convert the current to get steady low voltage current, impedance conversion circuits such as capacitive transformers, inductive transformers, and buck converter have been widely reported and made a positive progress. After that, we summarized the recent explorations in applications of TENG network and IC technology and exploited the potential of practical application of TENG-based energy harvesting system. Through integration and modular design and the comprehensive use of

PMC technology, the powering ability of the TENG-based energy harvesting system is expected to be further enhanced and the potential of its practical application is greatly improved. These works have made beneficial exploration for the output improvement and practical application of TENG, making it possible to applicate in the fields of IoT, wearable and implant devices.

Though considerable progress has been made in this field, there are still many challenges to be solved for the power management circuit of TENG. Firstly, further development of efficient power management circuits with low power consumption is necessary. This article reviews many circuit schemes with self-powered switches for control and demonstrates their feasibility. However, the power consumption of these schemes is still too high compared to the power output of the TENG. We believe that this problem can be solved from the aspects of circuit structure design and selection of low-power components. Secondly, the power management circuit needs a further exploration on scale and integration, which could further explore the potential for efficient energy output of TENG-based energy harvesting system. By combining different power management strategies, carrying out low-power design layout through IC technology, and docking with the load or energy storge devices, the charge loss of the whole process can be largely reduced and the practicability of the whole system can be also greatly enhanced. Finally, the performance of TENG and the corresponding energy storage unit needs to be further improved. Higher output of TENG allows more space for the circuit design, thus improving the overall energy transfer efficiency. Meanwhile, energy storage units that adapted to higher impedance inputs and unstable currents can further reduce charge loss, making practical applications of the system possible.

Acknowledgements

This work was funded by the National Key R&D Project from Minister of Science and Technology (No. 2021YFA1201602) and the National Natural Science Foundation of China (Nos. 52172203 and U21A20175).

References

[1] Gubbi, J.; Buyya, R.; Marusic, S.; Palaniswami, M. Internet of things (IoT): A vision, architectural elements, and future directions. *Fut. Gener. Comp. Syst.* **2013**, *29*, 1645–1660.

[2] Lee, I.; Lee, K. The internet of things (IoT): Applications, investments, and challenges for enterprises. *Bus. Horiz.* **2015**, *58*, 431–440.

[3] Zou, Y. J.; Raveendran, V.; Chen, J. Wearable triboelectric nanogenerators for biomechanical energy harvesting. *Nano Energy* **2020**, *77*, 105303.

[4] Wang, H. B.; Han, M. D.; Song, Y.; Zhang, H. X. Design, manufacturing and applications of wearable triboelectric nanogenerators. *Nano Energy* **2021**, *81*, 105627.

[5] Wang, Z. L. Self-powered nanotech. *Sci. Am.* **2008**, *298*, 82–87.

[6] Wang, Z. L. Triboelectric nanogenerators as new energy technology and self-powered sensors—Principles, problems and perspectives. *Faraday Discuss.* **2014**, *176*, 447–458.

[7] Hasan, M. A. M.; Wang, Y. H.; Bowen, C. R.; Yang, Y. 2D nanomaterials for effective energy scavenging. *Nano-Micro Lett.* **2021**, *13*, 82.

[8] Kim, W. G.; Kim, D. W.; Tcho, I. W.; Kim, J. K.; Kim, M. S.; Choi, Y. K. Triboelectric nanogenerator: Structure, mechanism, and applications. *ACS Nano* **2021**, *15*, 258–287.

[9] Choi, N. S.; Chen, Z. H.; Freunberger, S. A.; Ji, X. L.; Sun, Y. K.; Amine, K.; Yushin, G.; Nazar, L. F.; Cho, J.; Bruce, P. G. Challenges facing lithium batteries and electrical double-layer capacitors. *Angew. Chem., Int. Ed.* **2012**, *51*, 9994–10024.

[10] Kang, D. H. P.; Chen, M. J.; Ogunseitan, O. A. Potential environmental and human health impacts of rechargeable lithium batteries in electronic waste. *Environ. Sci. Technol.* **2013**, *47*, 5495–5503.

[11] Lee, J.; Urban, A.; Li, X.; Su, D.; Hautier, G.; Ceder, G. Unlocking the potential of cation-disordered oxides for rechargeable lithium batteries. *Science* **2014**, *343*, 519–522.

[12] Zi, Y. L.; Lin, L.; Wang, J.; Wang, S. H.; Chen, J.; Fan, X.; Yang, P. K.; Yi, F.; Wang, Z. L. Triboelectric-pyroelectric-piezoelectric hybrid cell for high-efficiency energy-harvesting and self-powered sensing. *Adv. Mater.* **2015**, *27*, 2340–2347.

[13] Gallup, D. L. Production engineering in geothermal technology: A review. *Geothermics* **2009**, *38*, 326–334.

[14] Boyaghchi, F. A.; Chavoshi, M.; Sabeti, V. Optimization of a novel combined cooling, heating and power cycle driven by geothermal and solar energies using the water/CuO (copper oxide) nanofluid. *Energy* **2015**, *91*, 685–699.

[15] Chen, N.; Liu, M. Y.; Zhou, W. D. Fouling and corrosion properties of SiO_2 coatings on copper in geothermal water. *Ind. Eng. Chem. Res.* **2012**, *51*, 6001–6017.

[16] Olasolo, P.; Juárez, M. C.; Morales, M. P.; D´Amico, S.; Liarte, I. A. Enhanced geothermal systems (EGS): A review. *Renew. Sust. Energ. Rev.* **2016**, *56*, 133–144.

[17] Lin, M. F.; Parida, K.; Cheng, X.; Lee, P. S. Flexible superamphiphobic film for water energy harvesting. *Adv. Mater. Technol.* **2017**, *2*, 1600186.

[18] Mehdizadeh, S.; Yasukawa, M.; Kuno, M.; Kawabata, Y.; Higa, M. Evaluation of energy harvesting from discharged solutions in a salt production plant by reverse electrodialysis (RED). *Desalination* **2019**, *467*, 95–102.

[19] Moran, E. F.; Lopez, M. C.; Moore, N.; Müller, N.; Hyndman, D. W. Sustainable hydropower in the 21st century. *Proc. Natl. Acad. Sci. USA* **2018**, *115*, 11891–11898.

[20] Xiong, J. Q.; Lin, M. F.; Wang, J. X.; Gaw, S. L.; Parida, K.; Lee, P. S. Wearable all-fabric-based triboelectric generator for water energy harvesting. *Adv. Energy Mater.* **2017**, *7*, 1701243.

[21] Yin, J.; Zhou, J. X.; Fang, S. M.; Guo, W. L. Hydrovoltaic energy on the way. *Joule* **2020**, *4*, 1852–1855.

[22] Zhang, Z. H.; Li, X. M.; Yin, J.; Xu, Y.; Fei, W. W.; Xue, M. M.; Wang, Q.; Zhou, J. X.; Guo, W. L. Emerging hydrovoltaic technology. *Nat. Nanotechnol.* **2018**, *13*, 1109–1119.

[23] Chen, B.; Yang, Y.; Wang, Z. L. Scavenging wind energy by triboelectric nanogenerators. *Adv. Energy Mater.* **2018**, *8*, 1702649.

[24] Perez, M.; Boisseau, S.; Gasnier, P.; Willemin, J.; Geisler, M.; Reboud, J. L. A cm scale electret-based electrostatic wind turbine for low-speed energy harvesting applications. *Smart Mater. Struct.* **2016**, *25*, 045015.

[25] Kwon, S. D. A T-shaped piezoelectric cantilever for fluid energy harvesting. *Appl. Phys. Lett.* **2010**, *97*, 164102.

[26] Fan, F. R.; Tian, Z. Q.; Wang, Z. L. Flexible triboelectric generator. *Nano Energy* **2012**, *1*, 328–334.

[27] Zhang, X. S.; Han, M. D.; Wang, R. X.; Zhu, F. Y.; Li, Z. H.; Wang, W.; Zhang, H. X. Frequency-multiplication high-output triboelectric nanogenerator for sustainably powering biomedical microsystems. *Nano Lett.* **2013**, *13*, 1168–1172.

[28] Bai, P.; Zhu, G.; Lin, Z. H.; Jing, Q. S.; Chen, J.; Zhang, G.; Ma, J. S.; Wang, Z. L. Integrated multilayered triboelectric nanogenerator for harvesting biomechanical energy from human motions. *ACS Nano* **2013**, *7*, 3713–3719.

[29] Kaltschmitt, M.; Streicher, W.; Wiese, A. *Renewable Energy: Technology, Economics and Environment*; Springer: Berlin, 2007.

[30] Beeby, S. P.; Tudor, M. J.; White, N. M. Energy harvesting vibration sources for microsystems applications. *Meas. Sci. Technol.* **2006**, *17*, R175–R195.

[31] Cheng, G.; Lin, Z. H.; Lin, L.; Du, Z. L.; Wang, Z. L. Pulsed nanogenerator with huge instantaneous output power density. *ACS Nano* **2013**, *7*, 7383–7391.

[32] Cheng, G.; Zheng, H. W.; Yang, F.; Zhao, L.; Zheng, M. L.; Yang, J. J.; Qin, H. F.; Du, Z. L.; Wang, Z. L. Managing and maximizing the output power of a triboelectric nanogenerator by controlled tip-electrode air-discharging and application for UV sensing. *Nano Energy* **2018**, *44*, 208–216.

[33] Qin, H.; Gu, G.; Shang, W.; Luo, H.; Zhang, W.; Cui, P.; Zhang, B.; Guo, J.; Cheng, G.; Du, Z. A universal and passive power management circuit with high efficiency for pulsed triboelectric nanogenerator. *Nano Energy* **2020**, *68*, 104372–104379.
[34] Zi, Y. L.; Niu, S. M.; Wang, J.; Wen, Z.; Tang, W.; Wang, Z. L. Standards and figure-of-merits for quantifying the performance of triboelectric nanogenerators. *Nat. Commun.* **2015**, *6*, 8376.
[35] Cheng, L.; Xu, Q.; Zheng, Y. B.; Jia, X. F.; Qin, Y. A self-improving triboelectric nanogenerator with improved charge density and increased charge accumulation speed. *Nat. Commun.* **2018**, *9*, 3773.
[36] Liu, W.; Wang, Z.; Wang, G.; Liu, G.; Chen, J.; Pu, X.; Xi, Y.; Wang, X.; Guo, H.; Hu, C. et al. Integrated charge excitation triboelectric nanogenerator. *Nat. Commun.* **2019**, *10*, 1426–1434.
[37] Xu, L.; Bu, T. Z.; Yang, X. D.; Zhang, C.; Wang, Z. L. Ultrahigh charge density realized by charge pumping at ambient conditions for triboelectric nanogenerators. *Nano Energy* **2018**, *49*, 625–633.
[38] Li, X.; Sun, Y. An SSHI rectifier for triboelectric energy harvesting. *IEEE Trans. Power Electron.* **2020**, *35*, 3663–3678.
[39] Ghaffarinejad, A.; Lu, Y.; Hinchet, R.; Galayko, D.; Hasani, J. Y.; Kim, S. W.; Basset, P. Bennet's doubler working as a power booster for triboelectric nano-generators. *Electron. Lett.* **2018**, *54*, 378–379.
[40] Pu, X.; Liu, M. M.; Li, L. X.; Zhang, C.; Pang, Y. K.; Jiang, C. Y.; Shao, L. H.; Hu, W. G.; Wang, Z. L. Efficient charging of Li-ion batteries with pulsed output current of triboelectric nanogenerators. *Adv. Sci.* **2016**, *3*, 1500255.
[41] Tang, W.; Zhou, T.; Zhang, C.; Fan, F. R.; Han, C. B.; Wang, Z. L. A power-transformed-and-managed triboelectric nanogenerator and its applications in a self-powered wireless sensing node. *Nanotechnology* **2014**, *25*, 225402.
[42] Xi, F. B.; Pang, Y. K.; Li, W.; Jiang, T.; Zhang, L. M.; Guo, T.; Liu, G. X.; Zhang, C.; Wang, Z. L. Universal power management strategy for triboelectric nanogenerator. *Nano Energy* **2017**, *37*, 168–176.
[43] Li, Q. Y.; Hu, Y. W.; Yang, Q. X.; Li, X. C.; Zhang, X. M.; Yang, H. K.; Ji, P. Y.; Xi, Y.; Wang, Z. L. A robust constant-voltage DC triboelectric nanogenerator using the ternary dielectric triboelectrification effect. *Adv. Energy Mater.* **2023**, *13*, 2202921.
[44] Pathak, M.; Kumar, R. Synchronous inductor switched energy extraction circuits for triboelectric nanogenerator. *IEEE Access* **2021**, *9*, 76938–76954.
[45] Niu, S.; Wang, X.; Yi, F.; Zhou, Y. S.; Wang, Z. L. A universal self-charging system driven by random biomechanical energy for sustainable operation of mobile electronics. *Nat. Commun.* **2015**, *6*, 8975–8984.
[46] Yoo, D.; Lee, S.; Lee, J.-W.; Lee, K.; Go, E. Y.; Hwang, W.; Song, I.; Cho, S. B.; Kim, D. W.; Choi, D. et al. Reliable DC voltage generation based on the enhanced performance triboelectric nanogenerator fabricated by nanoimprinting-poling process and an optimized high efficiency integrated circuit. *Nano Energy* **2020**, *69*, 104388–104399.
[47] Liang, X.; Jiang, T.; Feng, Y. W.; Lu, P. J.; An, J.; Wang, Z. L. Triboelectric nanogenerator network integrated with charge excitation circuit for effective water wave energy harvesting. *Adv. Energy Mater.* **2020**, *10*, 2002123.
[48] Niu, S. M.; Wang, S. H.; Lin, L.; Liu, Y.; Zhou, Y. S.; Hu, Y. F.; Wang, Z. L. Theoretical study of contact-mode triboelectric nanogenerators as an effective power source. *Energy Environ. Sci.* **2013**, *6*, 3576–3583.
[49] Niu, S. M.; Liu, Y.; Wang, S. H.; Lin, L.; Zhou, Y. S.; Hu, Y. F.; Wang, Z. L. Theory of sliding-mode triboelectric nanogenerators. *Adv. Mater.* **2013**, *25*, 6184–6193.
[50] Niu, S. M.; Liu, Y.; Wang, S. H.; Lin, L.; Zhou, Y. S.; Hu, Y. F.; Wang, Z. L. Theoretical investigation and structural optimization of single-electrode triboelectric nanogenerators. *Adv. Funct. Mater.* **2014**, *24*, 3332–3340.
[51] Niu, S. M.; Liu, Y.; Chen, X. Y.; Wang, S. H.; Zhou, Y. S.; Lin, L.; Xie, Y. N.; Wang, Z. L. Theory of freestanding triboelectric-layer-based nanogenerators. *Nano Energy* **2015**, *12*, 760–774.
[52] Wang, Z. L. On Maxwell's displacement current for energy and sensors: The origin of nanogenerators. *Mater. Today* **2017**, *20*, 74–82.
[53] Wang, Z. L. On the first principle theory of nanogenerators from Maxwell's equations. *Nano Energy* **2020**, *68*, 104272.
[54] Niu, S. M.; Wang, Z. L. Theoretical systems of triboelectric nanogenerators. *Nano Energy* **2015**, *14*, 161–192.
[55] Niu, S. M.; Zhou, Y. S.; Wang, S. H.; Liu, Y.; Lin, L.; Bando, Y.; Wang, Z. L. Simulation method for optimizing the performance of an integrated triboelectric nanogenerator energy harvesting system. *Nano Energy* **2014**, *8*, 150–156.
[56] Niu, S. M.; Liu, Y.; Zhou, Y. S.; Wang, S. H.; Lin, L.; Wang, Z. L. Optimization of triboelectric nanogenerator charging systems for efficient energy harvesting and storage. *IEEE Trans. Electron Devices* **2015**, *62*, 641–647.
[57] Shao, J. J.; Jiang, T.; Wang, Z. L. Theoretical foundations of triboelectric nanogenerators (TENGs). *Sci. China Technol. Sci.* **2020**, *63*, 1087–1109.
[58] Su, Y.; Xie, G.; Tai, H.; Li, S.; Yang, B.; Wang, S.; Zhang, Q.; Du, H.; Zhang, H.; Du, X. et al. Self-powered room temperature NO_2 detection driven by triboelectric nanogenerator under UV illumination. *Nano Energy* **2018**, *47*, 316–324.
[59] Zi, Y. L.; Wang, J.; Wang, S. H.; Li, S. M.; Wen, Z.; Guo, H. Y.; Wang, Z. L. Effective energy storage from a triboelectric nanogenerator. *Nat. Commun.* **2016**, *7*, 10987.
[60] Qin, H. F.; Cheng, G.; Zi, Y. L.; Gu, G. Q.; Zhang, B.; Shang, W. Y.; Yang, F.; Yang, J. J.; Du, Z. L.; Wang, Z. L. High energy storage efficiency triboelectric nanogenerators with unidirectional switches and passive power management circuits. *Adv. Funct. Mater.* **2018**, *28*, 1805216.
[61] Yang, J. J.; Yang, F.; Zhao, L.; Shang, W. Y.; Qin, H. F.; Wang, S. J.; Jiang, X. H.; Cheng, G.; Du, Z. L. Managing and optimizing the output performances of a triboelectric nanogenerator by a self-powered electrostatic vibrator switch. *Nano Energy* **2018**, *46*, 220–228.
[62] Xia, K. Q.; Wu, D.; Fu, J. M.; Xu, Z. W. A pulse controllable voltage source based on triboelectric nanogenerator. *Nano Energy* **2020**, *77*, 105112.
[63] Wang, H. M.; Xu, L.; Bai, Y.; Wang, Z. L. Pumping up the charge density of a triboelectric nanogenerator by charge-shuttling. *Nat. Commun.* **2020**, *11*, 4203.
[64] Hu, Y. W.; Li, Q. Y.; Long, L.; Yang, Q. X.; Fu, S. K.; Liu, W. L.; Zhang, X. M.; Yang, H. K.; Hu, C. G.; Xi, Y. Matching mechanism of charge excitation circuit for boosting performance of a rotary triboelectric nanogenerator. *ACS Appl. Mater. Interfaces* **2022**, *14*, 48636–48646.
[65] Guyomar, D.; Badel, A.; Lefeuvre, E.; Richard, C. Toward energy harvesting using active materials and conversion improvement by nonlinear processing. *IEEE Trans. Ultrason. Ferroelectr. Freq. Control* **2005**, *52*, 584–595.
[66] Peng, Y. M.; Choo, K. D.; Oh, S.; Lee, I.; Jang, T.; Kim, Y.; Lim, J.; Blaauw, D.; Sylvester, D. An efficient piezoelectric energy harvesting interface circuit using a sense-and-set rectifier. *IEEE J. Solid State Circuits* **2019**, *54*, 3348–3361.
[67] Ramadass, Y. K.; Chandrakasan, A. P. An efficient piezoelectric energy harvesting interface circuit using a bias-flip rectifier and shared inductor. *IEEE J. Solid State Circuits* **2010**, *45*, 189–204.
[68] Khushboo; Azad, P. Design and analysis of a synchronized interface circuit for triboelectric energy harvesting. *J. Electron. Mater.* **2020**, *49*, 2491–2501.
[69] Kara, I.; Becermis, M.; Kamar, M. A. A.; Aktan, M.; Dogan, H.; Mutlu, S. A 70-to-2 V triboelectric energy harvesting system utilizing parallel-SSHI rectifier and DC-DC converters. *IEEE Trans. Circuits Syst. I Regul. Pap.* **2021**, *68*, 210–223.
[70] Le, T. T.; Han, J. F.; Jouanne, A. V.; Mayaram, K.; Fiez, T. S. Piezoelectric micro-power generation interface circuits. *IEEE J. Solid-State Circuits* **2006**, *41*, 1411–1420.
[71] Dallago, E.; Frattini, G.; Miatton, D.; Ricotti, G.; Venchi, G. Integrable high-efficiency AC-DC converter for piezoelectric energy scavenging system. In *Proceedings of the 2017 IEEE International Conference on Portable Information Devices*, Orlando, FL, USA, 2007, pp 1–5.
[72] De Queiroz, A. C. M. Variations of the doubler of electricity. *Phys. Educ.* **2019**, *54*, 035019.

[73] Ghaffarinejad, A.; Hasani, J. Y.; Hinchet, R.; Lu, Y. X.; Zhang, H. M.; Karami, A.; Galayko, D.; Kim, S. W.; Basset, P. A conditioning circuit with exponential enhancement of output energy for triboelectric nanogenerator. *Nano Energy* **2018**, *51*, 173–184.

[74] Wang, H.; Zhu, J. X.; He, T. Y. Y.; Zhang, Z. X.; Lee, C. K. Programmed-triboelectric nanogenerators—A multi-switch regulation methodology for energy manipulation. *Nano Energy* **2020**, *78*, 105241.

[75] Zhang, H. M.; Lu, Y. X.; Ghaffarinejad, A.; Basset, P. Progressive contact-separate triboelectric nanogenerator based on conductive polyurethane foam regulated with a Bennet doubler conditioning circuit. *Nano Energy* **2018**, *51*, 10–18.

[76] Wang, J. L.; Li, Y. K.; Xie, Z. J.; Xu, Y. H.; Zhou, J. W.; Cheng, T. H.; Zhao, H. W.; Wang, Z. L. Cylindrical direct-current triboelectric nanogenerator with constant output current. *Adv. Energy Mater.* **2020**, *10*, 1904227.

[77] Liu, D.; Yin, X.; Guo, H. Y.; Zhou, L. L.; Li, X. Y.; Zhang, C. L.; Wang, J.; Wang, Z. L. A constant current triboelectric nanogenerator arising from electrostatic breakdown. *Sci. Adv.* **2019**, *5*, eaav6437.

[78] Zhao, Z. H.; Dai, Y. J.; Liu, D.; Zhou, L. L.; Li, S. X.; Wang, Z. L.; Wang, J. Rationally patterned electrode of direct-current triboelectric nanogenerators for ultrahigh effective surface charge density. *Nat. Commun.* **2020**, *11*, 6186.

[79] Zhu, G.; Chen, J.; Zhang, T. J.; Jing, Q. S.; Wang, Z. L. Radial-arrayed rotary electrification for high performance triboelectric generator. *Nat. Commun.* **2014**, *5*, 3426.

[80] Han, C. B.; Zhang, C.; Tang, W.; Li, X. H.; Wang, Z. L. High power triboelectric nanogenerator based on printed circuit board (PCB) technology. *Nano Res.* **2015**, *8*, 722–730.

[81] Zhai, N. N.; Wen, Z.; Chen, X. P.; Wei, A. M.; Sha, M.; Fu, J. J.; Liu, Y. N.; Zhong, J.; Sun, X. H. Blue energy collection toward all-hours self-powered chemical energy conversion. *Adv. Engergy Mater.* **2020**, *10*, 2001041.

[82] Wang, Z.; Liu, W.; He, W.; Guo, H.; Long, L.; Xi, Y.; Wang, X.; Liu, A.; Hu, C. Ultrahigh electricity generation from low-frequency mechanical energy by efficient energy management. *Joule* **2021**, *5*, 441–455.

[83] Zi, Y. L.; Guo, H. Y.; Wang, J.; Wen, Z.; Li, S. M.; Hu, C. G.; Wang, Z. L. An inductor-free auto-power-management design built-in triboelectric nanogenerators. *Nano Energy* **2017**, *31*, 302–310.

[84] Liu, W. L.; Wang, Z.; Wang, G.; Zeng, Q. X.; He, W. C.; Liu, L. Y.; Wang, X.; Xi, Y.; Guo, H. Y.; Hu, C. G. et al. Switched-capacitor-convertors based on fractal design for output power management of triboelectric nanogenerator. *Nat. Commun.* **2020**, *11*, 1883.

[85] Park, I.; Maeng, J.; Shim, M.; Jeong, J.; Kim, C. A high-voltage dual-input buck converter achieving 52.9% maximum end-to-end efficiency for triboelectric energy-harvesting applications. *IEEE J. Solid State Circuits* **2020**, *55*, 1324–1336.

[86] Ottman, G. K.; Hofmann, H. F.; Lesieutre, G. A. Optimized piezoelectric energy harvesting circuit using step-down converter in discontinuous conduction mode. *IEEE Trans. Power Electron.* **2003**, *18*, 696–703.

[87] Harmon, W.; Bamgboje, D.; Guo, H. Y.; Hu, T. S.; Wang, Z. L. Self-driven power management system for triboelectric nanogenerators. *Nano Energy* **2020**, *71*, 104642.

[88] Liang, X.; Jiang, T.; Liu, G. X.; Xiao, T. X.; Xu, L.; Li, W.; Xi, F. B.; Zhang, C.; Wang, Z. L. Triboelectric nanogenerator networks integrated with power management module for water wave energy harvesting. *Adv. Funct. Mater.* **2019**, *29*, 1807241.

[89] Park, I.; Maeng, J.; Shim, M.; Jeong, J.; Kim, C. A bidirectional high-voltage dual-input buck converter for triboelectric energy-harvesting interface achieving 70.72% end-to-end efficiency. In *Proceedings of the 2019 Symposium on VLSI Circuits*, Kyoto, Japan, 2019, pp C326–C327.

[90] Zhang, H. M.; Galayko, D.; Basset, P. A self-sustained energy storage system with an electrostatic automatic switch and a buck converter for triboelectric nanogenerators. *J. Phys. Conf. Ser.* **2019**, *1407*, 012016–012020.

[91] Liang, X.; Liu, Z. R.; Feng, Y. W.; Han, J. J.; Li, L. L.; An, J.; Chen, P. F.; Jiang, T.; Wang, Z. L. Spherical triboelectric nanogenerator based on spring-assisted swing structure for effective water wave energy harvesting. *Nano Energy* **2021**, *83*, 105836–105844.

[92] Khan, M. B.; Kim, D. H.; Han, J. H.; Saif, H.; Lee, H.; Lee, Y.; Kim, M.; Jang, E.; Hong, S. K.; Joe, D. J. et al. Performance improvement of flexible piezoelectric energy harvester for irregular human motion with energy extraction enhancement circuit. *Nano Energy* **2019**, *58*, 211–219.

[93] Luo, L.; Bao, D.; Yu, W.; Zhang, Z.; Ren, T. A power manager system with 78% efficiency for high-voltage triboelectric nanogenerators. *Sci. China Inf. Sci.* **2017**, *60*, 029401: 1–029401: 3.